# THE PRODUCTION OF ELLIPTIC INTERFERENCES IN RELATION TO INTERFEROMETRY

By CARL BARUS
*Hazard Professor of Physics, Brown University*

WASHINGTON, D. C.
Published by the Carnegie Institution of Washington
1911

# THE PRODUCTION OF ELLIPTIC INTERFERENCES IN RELATION TO INTERFEROMETRY

By CARL BARUS

*Hazard Professor of Physics, Brown University*

WASHINGTON, D. C.

Published by the Carnegie Institution of Washington

1911

CARNEGIE INSTITUTION OF WASHINGTON

Publication No. 149

PRESS OF J. B. LIPPINCOTT COMPANY
PHILADELPHIA, PA.

# PREFACE.

In connection with my work on the coronas as a means for the study of nucleation, I came across a principle of interferometry which seemed of sufficient importance to justify special investigation. This has been undertaken in the following chapters, and what appears to be a new procedure in interferometry of great promise and varied application has been developed. In case of the coronas there is a marked interference phenomenon superposed on the diffractions. The present method is therefore to consist in a simplification or systematization of this effect, by bringing two complete component diffraction spectra, from the same source of light, to interfere. This may be done in many ways, either directly, or with a halved transmission or reflecting grating, or by using modifications of the devices of Jamin, Michelson, and others for separating the components.

In the direct method, chapters II and III, a mirror immediately behind the grating returns the reflected-diffracted and diffracted-reflected rays, to be superimposed for interference, producing a series of phenomena which are eminently useful, in addition to their great beauty. In fact the interferometer so constructed needs but ordinary plate glass and replica gratings. It gives equidistant fringes, rigorously straight, and their distance apart and inclination are thus measurable by ocular micrometry. The fringes are duplex in character and an adjustment may be made whereby ten small fringes occupy the same space in the field as one large fringe, so that sudden expansions within the limits of the large fringe (as for instance in magnetostriction) are determinable. This has not been feasible heretofore. Length and small angles (seconds of arc) are thus subject to micrometric measurement. Finally the interferences are very easily produced and are strong with white light, while the spectrum line may be kept in the field as a stationary landmark. The limiting sensitiveness is half the wave-length of light.

The theory of these phenomena has been worked out in its practical bearings, advantageous instrumental equipment has been discussed, and a number of incidental applications to test the apparatus have been made. In much of this work, including that of the first chapter on a modification of Rowland's spectrometer, I had the assistance of my son, Mr. Maxwell Barus, before he entered into the law.

The range of measurement of an instrument like the above is necessarily limited to about 1 cm. and the component rays are not separated. To increase the range indefinitely and to separate the component rays, the grating may replace the symmetrically oblique transparent mirror of

Michelson's adjustment, for instance. In this way transmitted-reflected-diffracted and reflected-transmitted-diffracted spectra, or two corresponding diffracted spectra returned by the opaque mirrors $M$ and $N$, may be brought to interfere. In both cases the experiments as detailed in chapters IV and V have been strikingly successful. The interference pattern, however, is now of the ring type, extending throughout the whole spectrum from red to violet with the fixed spectrum lines simultaneously in view. These rings closely resemble confocal ellipses, and their centers have the same position in all orders of spectra; but the major axes of the ellipses are liable to be vertical in the first and horizontal in all the higher orders of spectra.

Again there is an opportunity for coarse and fine adjustment, inasmuch as the rings have the usual sensitive radial motion, as the virtual air-space increases or decreases, while the centers simultaneously *drift* as a whole, across the fixed lines of the spectrum, from the red to the violet end.

Drift and radial motion may be regulated in any ratio. The general investigation shows that three groups, each comprising a variety of interferences, are possible and I have worked out the practical side of the theory of the phenomenon. Transparent silvered surfaces are superfluous, as the ellipses are sufficiently strong to need no accessory treatment. Considerable width of spectrum slit is also admissible. Finally, the ellipses may be made of any size and the sensitiveness of their lateral motion may be regulated to any degree by aid of a compensator. In this adjustment the drift may be made even more delicate than the radial motion, thus constituting a new feature in interferometry.

The interesting result follows from the work that the displacement of the centers of ellipses does not correspond to the zero of path difference, but to an adjustment in which $\mu-\lambda d\mu/d\lambda$ (where $\mu$ is the index of refraction and $\lambda$ the wave-length) is critical.

It is obvious that the transparent plate grating may be replaced by a reflecting grating. Thus the grating may be replaced by a plate of glass, as in Michelson's case, and the function of the two opaque mirrors may be performed by two identical plane *reflecting* gratings, each symmetrically set at the diffraction angle of the spectrum to the incident ray. In this case the undeviated reflection is thrown out, whereas the spectra overlap in the telescope. Finally the grating may itself be cut in half by a plane parallel to the rulings, whereupon the two overlapping spectra will interfere elliptically, if by a micrometer one-half is slightly moved, parallel to itself, out of the original common vertical plane of the grating.

Throughout the editorial work and in the drawings I have profited by the aptitude and tireless efficiency of my former student, Miss Ada I. Burton. But for her self-sacrificing assistance it would have been difficult to bring the present work to completion.

CARL BARUS.

BROWN UNIVERSITY, PROVIDENCE, RHODE ISLAND.

# CONTENTS.

Chapter I.—*On an Adjustment of the Plane Grating Similar to Rowland's method for the Concave Grating.* By C. Barus and M. Barus.



Chapter II.—*The Interference of the Reflected-Diffracted and the Diffracted-Reflected Rays of a Plane Transparent Grating, and on an Interferometer.* By C. Barus and M. Barus.



Chapter III.—*The Grating Interferometer.* By C. Barus and M. Barus.



Chapter IV.—*The Use of the Grating in Interferometry; Experimental Results.*



Chapter V.—*Interferometry with the Aid of the Grating; Theoretical Results.*

PART I. INTRODUCTION.

PART II. DIRECT CASES OF INTERFERENCE. DIFFRACTION ANTECEDENT.



PART III. DIRECT CASES OF INTERFERENCE. REFLECTION ANTECEDENT.



PART IV. INTERFERENCES IN GENERAL, AND SUMMARY.

# CHAPTER I.

## ON AN ADJUSTMENT FOR THE PLANE GRATING SIMILAR TO ROWLAND'S METHOD FOR THE CONCAVE GRATING. By C. Barus and M. Barus.

**1. Apparatus.**—The remarkable refinement which has been attained (notably by Mr. Ives and others) in the construction of celluloid replicas of the plane grating makes it desirable to construct a simple apparatus whereby the spectrum may be shown and the measurement of wave-length made, in a way that does justice to the astonishing performance of the grating. We have therefore thought it not superfluous to devise the following inexpensive contrivance, in which the wave-length is strictly proportional to the shift of the carriage at the eyepiece; which for the case of a good 2-meter scale divided into centimeters admits of a measurement of wave-length to a few Angström units and with a millimeter scale should go much further.

Observations are throughout made on both sides of the incident rays and from the mean result most of the usual errors should be eliminated by symmetry. It is also shown that the symmetrical method may be adapted to the concave grating.

In fig. 1 *A* and *B* are two double slides, like a lathe bed, 155 cm. long and 11 cm. apart, which happened to be available for optical purposes, in the laboratory. They were therefore used, although single slides at right angles to each other, similar to Rowland's, would have been preferable. The carriages *C* and *D*, 30 cm. long, kept at a fixed distance apart by the rod *ab*, are in practice a length of ¼-inch gas pipe, swiveled at *a* and *b*, 169.4 decimeters apart, and capable of sliding right and left and to and fro, normally to each other.

The swiveling joint, which functioned excellently, is made very simply of ¼-inch gas-pipe tees and nipples, as shown in fig. 2. The lower nipple *N* is screwed tight into the T, but all but tight into the carriage *D*, so that the rod *ab* turns in the screw *N*, kept oiled. Similarly the nipple *N''* is either screwed tight into the T (in one method, revolvable grating), or all but tight (in another method, stationary grating), so that the table *tt*, which carries the grating *g*, may be fixed while the nipple *N''* swivels in the T.

Any ordinary laboratory clamp *K* and a similar one on the upright *C* (screwed into the carriage *D*) secures a small rod *k* for this purpose. Again a hole may be drilled through the standards at *K* and *C* and provided with set screws to fix a horizontal rod *k* or check. The rod, *k*, should be long enough to similarly fix the standard on the slide *S*, carrying the slit, and be prolonged further toward the rear to carry the flame or Geissler tube apparatus. The table *tt* is revoluble on a brass rod fitting within the gas pipe, which has been slotted across so that the conical nut *M* may hold it firmly. The axis passes through the middle of the grating, which is fastened centrally to the table *tt* with the usual tripod adjustment.

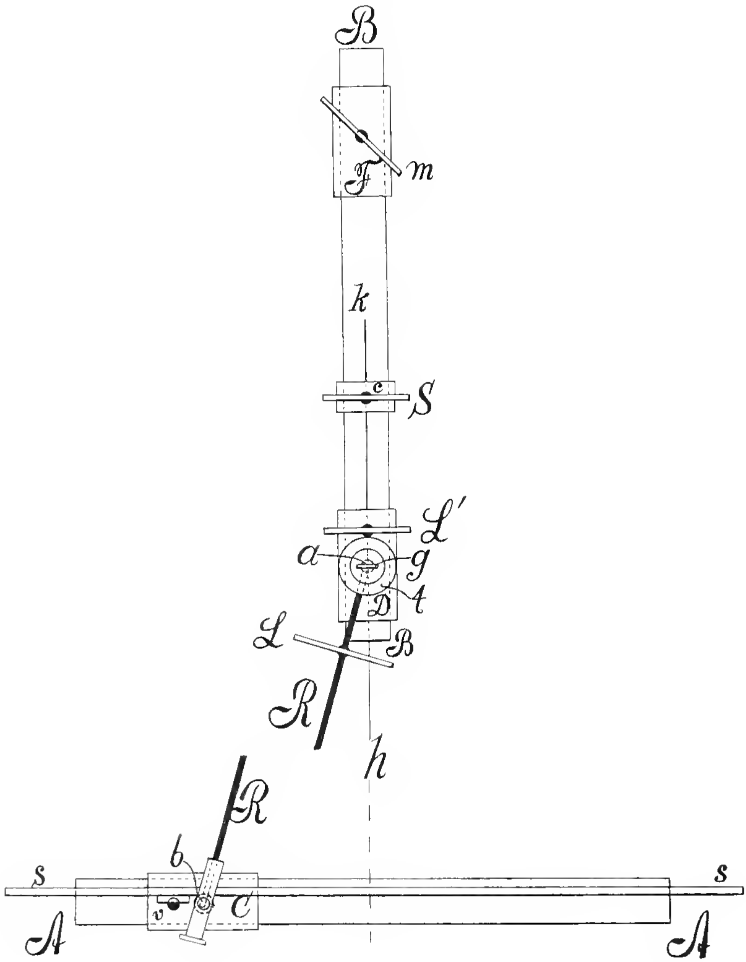


FIG. 1.—Plan of the apparatus.

**2. Single focussing lens in front of grating.**—I shall describe three methods in succession, beginning with the first. Here a large lens *L*, of about 56 cm. focal distance and about 10 cm. in diameter, is placed just in front of the grating, properly screened and throwing an image of the slit *S* upon the cross-hairs of the eyepiece *E*, the line of sight of which is always parallel to the rod *ab*, the end *b* swiveled in the carriage *C*, as stated. (See fig. 2.) An ordinary lens of 5 to 10 cm. focal distance, with an appropriate diaphragm, is adequate and in many ways preferable to stronger eyepieces. The slit, *S*, carried on its own slide and capable of being clamped to *C* when necessary, as stated, is additionally provided with a long rod *hh* lying underneath the carriage, so that the slit *S* may be put accurately in focus by the observer at *C*. *F* is a carriage for the mirror or the flame or other source of light whose spectrum is to be examined; or the source may be adjustable on the rear of the rod by which *D* and *S* are locked together.

Finally, the slide *AB* is provided with a scale *ss* and the position of the carriage *C* read off by aid of the vernier *v*. A good wooden scale, graduated in centimeters, happened to be available, the vernier reading to within one millimeter. For more accurate work a brass scale in millimeters with an appropriate vernier has since been provided.

Eyepiece *E*, slit *S*, flame *F*, etc., may be raised and lowered by the split tube device shown as at *M* and *M′* in fig. 2.

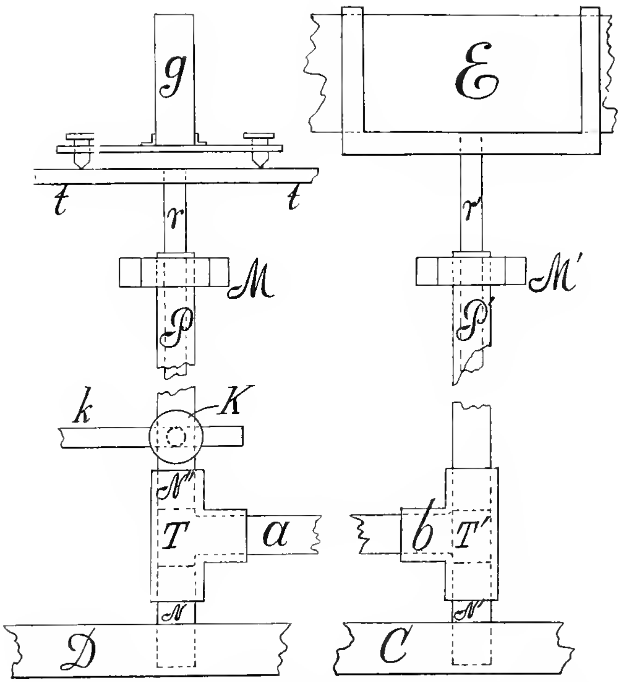


FIG. 2.—Elevation of standards of grating (*g*) and eyepiece (*E*).

**3. Adjustments.**—The first general test which places slit, grating and its spectra, and the two positions of the eyepiece in one plane, is preferably made with a narrow beam of sunlight, though lamplight suffices in the dark. Thereafter let the slit be focussed with the eyepiece on the right, marking the position of the slit; next focus the slit for the eyepiece on the left; then place the slit midway between these positions and now focus by slowly rotating the grating. The slit will then be found in focus for both positions and the grating which acts as a concave lens counteracting $L$ will be symmetrical with respect to both positions. Let the grating be thus adjusted when fixed normally to the slide $B$ or parallel to $A$. Then for the first order of the spectra the wave-length $\lambda = d \sin \theta$, where $d$ is the grating space and $\theta$ the angle of diffraction. The angle of incidence $i$ is zero.

Again let the grating adjusted for symmetry be free to rotate with the rod $ab$. Then $\theta$ is zero and $\lambda = d \sin i$.

In both cases, however, if $2x$ be the distance apart of the carriage $C$, measured on the scale $ss$, for the effective length of rod $ab = r$ between axis and axis,

$$\lambda = dx/r \text{ or } (d/2r)2x$$

so that in either case $\lambda$ and $x$ are proportional quantities.

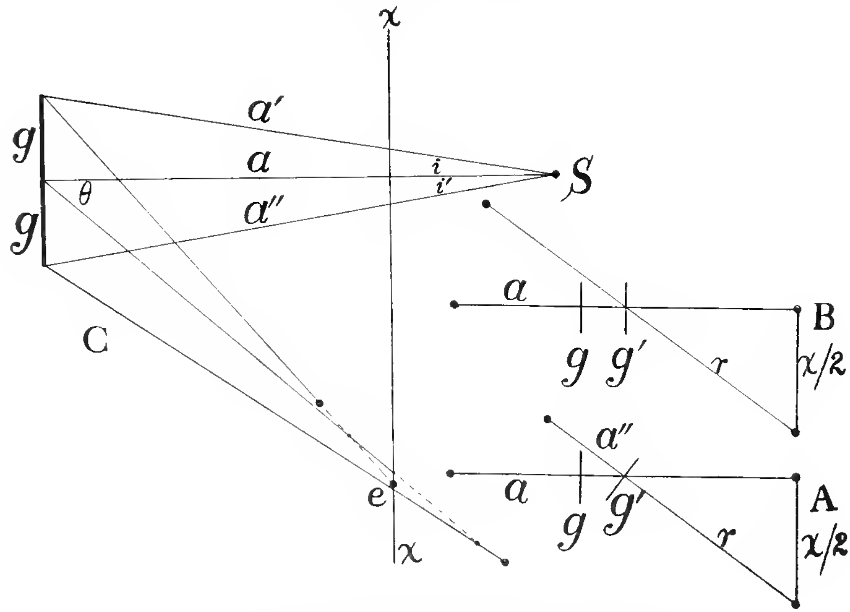


FIG. 3.—A, B, C, Diagrams relative to conjugate foci.

The whole spectrum is not, however, clearly in focus at one time, though the focussing by aid of the rod $hh$ is not difficult. For extreme positions a pulley adjustment, operating on the ends of $h$, is a convenience, the cords running around the slide $AA$. In fact if the slit is in focus when the eye-piece is at the center ($\theta = o$, $i = o$), at a distance $a$ from the grating, then for the fixed grating, fig. 4,

$$a' = a \frac{r^2}{r^2 - x^2}$$

where $a'$ is the distance between grating and slit for the diffraction corresponding to $x$. Hence the focal distance of the grating regarded as a concave lens is $f' = ar^2/x$. For the fixed grating and a given color, it frequently happens that the undeviated ray and the diffracted rays of the same color are simultaneously in focus, though this does not follow from the equation.

Again for the rotating grating, fig. 3A, if $a''$ is the distance between slit and grating $a''=a\frac{r^2-x^2}{r^2}$, so that its focal distance is $f''=a\frac{r^2-x^2}{x^2}$. It follows also that $a'\times a''=a$. For $a=80$ cm. and sodium light, the adjustment showed roughly $f'=650$ cm., $f''=570$ cm., the behavior being that of a weak concave lens. The same $a=80$ cm. and sodium light showed furthermore $a'=91$ and $a''=70.3$.

Finally there is a correction needed for the lateral shift of rays, due to the fact that the grating film is inclosed between two moderately thick

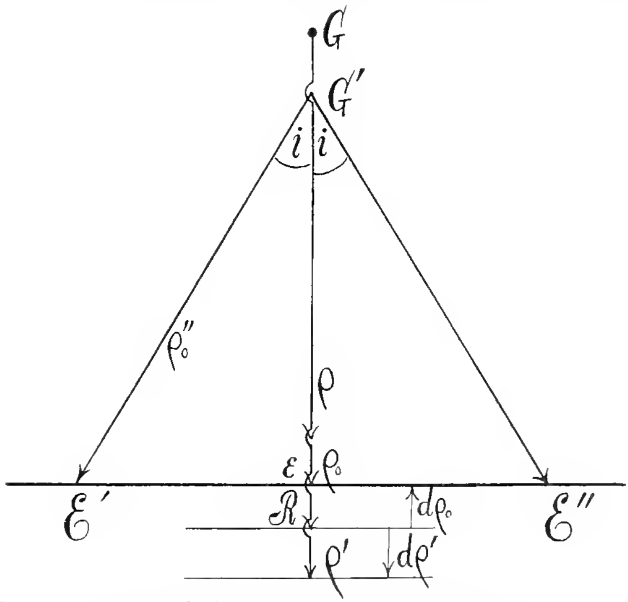


FIG. 4.—Diagram of adjustment for concave grating. $R$, $\rho_0$, and $\rho'$ are measured from $G$, $\rho$ and $\rho_0''$ from $G'$.

plates of glass (total thickness $t=.99$ cm.) of the index of refraction $n$. This shift thus amounts to

$$e=\frac{tx}{r}\left(\frac{1}{\sqrt{1-x^2/r^2}}-\frac{1}{\sqrt{n^2-x^2/r^2}}\right)\frac{b}{a}$$

But since this shift is on the rear side of the lens $L$, its effect on the eyepiece beyond will be (if $f$ is the principal focal distance and $b$ the conjugate focal distance between lens and eyepiece, remembering that the shift must be resolved parallel to the scale $ss$)

$$e=\frac{tx}{r}\left(\frac{1}{\sqrt{1-x^2/r^2}}-\frac{1}{\sqrt{n^2-x^2/r^2}}\right)\left(\frac{b}{f}-1\right)$$

where the correction $e$ is to be added to $2x$, and is positive for the rotating grating and negative for the stationary grating.

Hence in the mean values of $2x$ for stationary and rotating grating the effect of $e$ is eliminated. For a given lens at a fixed distance from the eye-piece $(b/f-1)$ is constant.

**4. Data for single lens in front of grating.**—In conclusion we select a few results taken at random from the notes.

TABLE 1.

| Stationary grating. | | | | Rotating grating. | | | |
|---|---|---|---|---|---|---|---|
| Line. | Observed $2x'$ | Shift. | Corrected $2x$ | Line. | Observed $2x'$ | Shift. | Corrected $2x$ |
| C........ | 132.60 | −.26 | 132.34 | C........ | 132.10 | +.26 | 132.36 |
| $D_2$....... | 118.90 | −.23 | 118.67 | $D_2$....... | 118.45 | .23 | 118.68 |
| F........ | 98.23 | −.19 | 98.04 | F........ | 97.90 | .19 | 98.09 |
| Hydrogen violet.. | 87.87 | −.16 | 87.71 | Hydrogen violet.. | 87.50 | .16 | 87.66 |

The real test is to be sought in the corresponding values of $2x$ for the stationary and rotating cases, and these are very satisfactory, remembering that a centimeter scale on wood with a vernier reading to millimeters only was used for measurement.

**5. Single focussing lens behind the grating.**—The lens $L$, which should be achromatic, is placed in the standard $C$. The light which passes through the grating is now convergent, whereas it was divergent in §2. Hence the focal points at distances $a'$, $a''$ lie in front of the grating; but in other respects the conditions are similar but reversed. Apart from signs,

$$a'=a\frac{r^2-x^2}{r^2}, \text{ for the stationary grating}$$

$$a''=a\frac{r^2}{r^2-x^2}, \text{ for the rotating grating}$$

The correction for shift loses the factor $(b/f-1)$ and becomes

$$e=\frac{tx}{r}\left(\frac{1}{\sqrt{1-x^2/r^2}}-\frac{1}{\sqrt{n^2-x^2/r^2}}\right)$$

As intimated, it is negative for the rotating grating and positive for the stationary grating. It is eliminated in the mean values.

**6. Data for single lens behind the grating.**—An example of the results will suffice. Different parts of the spectrum require focussing.

TABLE 2.

| Grating. | Line. | $2x'$ | Shift. | $2x$ |
|---|---|---|---|---|
| Stationary....... | $D_2$ | 118.40 | +.13 | 118.53 |
| Rotating........ | $D_2$ | 118.65 | −.13 | 118.52 |

The values of $2x$, remembering that a centimeter scale was used, are again surprisingly good. The shift is computed by the above equation. It may be eliminated in the mean of the two methods. The lens $L'$ at $C$ may be more easily and firmly fixed than at $L$.

**7. Collimator method.**—The objection to the above single-lens methods is the fact that the whole spectrum is not in sharp focus at once. Their advantage is the simplicity of the means employed. If lenses at $L'$ and at $L$ are used together, the former as a collimator (achromatic) and with a focal distance of about 50 cm., and the latter (focal distance to be large, say 150 cm.) as the objective of a telescope, all the above difficulties disappear and the magnification may be made even excessively large. The whole spectrum is brilliantly in focus at once and the corrections for the shift of lines due to the plates of the grating vanish. Both methods for stationary and rotating gratings give identical results. The adjustments are easy and certain, for with sunlight (or lamplight in the dark) the image of the slit may be reflected back from the plate of the grating on the plane of the slit itself, while at the same time the transmitted image may be equally sharply adjusted on the focal plane of the eyepiece. It is therefore merely necessary to place the plane of spectra horizontal. Clearly $a'$ and $a''$ are all infinite.

In this method the slides $S$ and $D$ are clamped at the focal distance apart, so that flame, etc., slit, collimator lens, and grating move together. The grating may or may not be revoluble with the lens $L$ on the axis $a$.

**8. Data for the collimator method.**—The following data chosen at random may be discussed. The results were obtained at different times and under different conditions. The grating nominally contained about 15,050 lines per inch. The efficient rod-length $ab$ was $R=169.4$ cm. Hence if $1/C=15{,}050\times.3937\times338.8$, the wave-length $\lambda-C=2x$ cm.

TABLE 3.—Stationery rotating grating.

| Lines. | $2x'$ | $2x$ |
|---|---|---|
| $D_2$ ....... | { 118.30<br>118.08 } | 118.19 |
| $D_2$ ....... | { 118.27<br>118.05 } | 118.16 |

Rowland's value of $D_2$ is $58.92\times10^{-6}$ cm.; the mean of the two values of $2x$ just stated will give $58.87\times10^{-6}$ cm. The difference may be due either to the assumed grating-space, or to the value of $R$ inserted, neither of which was reliable absolutely to much within 0.1 per cent.

Curiously enough, an apparent shift effect remains in the values of $2x$ for stationary and rotating grating, as if the collimation were imperfect. The reason for this is not clear, though it must in any case be eliminated in the mean result. Possibly the friction involved in the simultaneous motion of three slides is not negligible and may leave the system under slight strain equivalent to a small lateral shift of the slit.

**9. Discussion.**—The chief discrepancy is the difference of values for $2x$ in the single-lens system (for $D_2$, 118.7 and 118.5 cm., respectively) as compared with a double-lens system (for $D_2$, 118.2 cm.) amounting to 0.2 to 0.4 per cent. For any given method this difference is consistently maintained. It does not therefore seem to be mere chance.

We have for this reason computed all the data involved for a fixed grating 5 cm. in width, in the two extreme positions, fig. 3, C, the ray being normally incident at the left-hand and the right-hand edges, respectively, for the method of § 6. The meaning of the symbols is clear from fig. 3, C, $S$ being the virtual source, $g$ the grating, $e$ the diffraction conjugate focus of $S$ for normal incidence, so that $b=r$ is the fixed length of rod carrying grating and eyepiece. It is almost sufficient to assume that all diffracted rays $b'$ to $b''$ are directed toward $e$, in which case equation (1) would hold; but this will not bring out the divergence in question. They were therefore not used. Hence the following equations (2) to (5) successively apply where $d$ is the grating space.

$$\cot\theta' = (b/g + \sin\theta)/\cos\theta; \quad \cot\theta'' = (b/g - \sin\theta)/\cos\theta \tag{1}$$

$$a = b/\cos^2\theta; \quad a' = a'' = \sqrt{g^2 + a^2} \tag{2}$$

$$\sin i' = \sin i'' = g/a' \tag{3}$$

$$-\sin i' + \sin(\theta+\theta') = \lambda/d; \; \sin\theta = \lambda/d; \; \sin i'' + \sin(\theta+\theta'') = \lambda/d \tag{4}$$

$$\cos^2 i'/a' = \cos^2(\theta+\theta')b'; \quad \cos^2 i''/a'' = \cos^2(\theta+\theta'')/b'' \tag{5}$$

Since $\theta$, $g$, $\lambda$, $d$, $b$ are given, $\theta'$ and $\theta''$ are found in equation (4), apart from signs. If $\delta_1'$ and $\delta_1''$ be the distance apart of the projections of the extremities of $b'$ and $b$, $b$ and $b''$, respectively, on the line $x$,

$$\delta_1' = g + (b - b')\sin\theta - b'\sin i' \qquad \delta_1'' = g + (b'' - b)\sin\theta - b''\sin i'' \tag{6}$$

If $\delta_2'$ and $\delta_2''$ be the distance apart of the intersections of the prolongation of $b'$ and $b$, $b$ and $b''$, respectively, with the line $x$

$$\left.\begin{aligned}\delta_2' &= \sin(\theta+\theta')(b\cos\theta/\cos(\theta+\theta') - b')\\ \delta_2'' &= \sin(\theta-\theta'')(b'' - b\cos\theta/\cos(\theta-\theta''))\end{aligned}\right\} \tag{7}$$

Given $b=169.4$ cm., $\theta = 20°\ 22'$, about for sodium, $g=5$ cm., the following values are obtained:

| | | | |
|---|---|---|---|
| $\theta' = 1°36'$ | $a = 192.7$ cm. | $\theta'' = 1°34'$ | $a' = a'' = 192.8$ cm. |
| $i' = i'' = 1°30'$ | $b' = 166.0$ cm. | $r = b = 169.4$ cm. | $b'' = 172.4$ cm. |

whence

$$\delta_1' = 1.92 \text{ cm.} \qquad \delta_2'' = 1.74 \text{ cm.}$$

These limits are surprisingly wide. If, however, they should be quite wiped out on focussing, for any group of rays and symmetrical observations on the two sides of the apparatus, this would be no source of discrepancy. The effect of focussing the two parts of the grating may, in the first instance, be considered as a prolongation of $b'$ till it cuts $x$, together with the corresponding points for the intersection of $b''$ with $x$. Thus the values $\delta_2'$ and $\delta_2''$ are here in question and they are

$$\delta_2' = 1.97 \text{ cm.} \qquad \delta_2' - \delta_1' = .05 \text{ cm.}$$

whence

$$\delta_2'' = 1.65 \text{ cm.} \qquad \delta_1'' = \delta_2 = .09 \text{ cm.}$$

are the conjugate foci for the extreme rays of the grating, respectively, beyond the conjugate focus of the middle or normal rays $b$, on $x$. Hence the mean of the extreme rays lies at .07 cm. beyond (greater $\theta$) the normal ray, and the $\lambda$ found in the first instance is too large as compared with the true value for the normal ray.

The datum .07 cm. may be taken as the excess of $2x$, corresponding to the excess of angle for a grating one-half as wide and observed on both sides ($2x$), as was actually the case. Finally, since not the whole of the grating is not in focus at once a correction less than .07 cm. for $2x$ must clearly be in question. This is quite below the difference of several millimeters brought out in §§4 and 6.

To make this point additionally sure and avoid the assumption of the last paragraph, we will compute the conjugate focus of the central ray (different angles $\theta$) on the $b'$ focal plane parallel to the grating and to $x$ and on the $b''$ focal plane parallel to $x$. The computation is simpler if the central ray is thus focussed than if the extreme rays are focussed on the $x$ plane. The distance apart will be

$$\delta_3' = g - b' \cos(\theta + \theta')(\tan(\theta + \theta') - \tan\theta)$$
$$\delta_3'' = g - b'' \cos(\theta - \theta'')(\tan\theta - \tan(\theta - \theta''))$$

Inserting the results for $\theta \quad \theta_1' \quad \theta_1'' \quad b' \quad b'' \quad g$

$$\delta_3' = .06 \qquad \delta_3'' = -.04$$

Both the $b$ foci thus correspond to large angles. Their mean, however, may be considered as vanishing on the intermediate $x$ plane.

Thus it is clear that the effect of focussing is without influence on the diffraction angle and much within the limits of observation. It is therefore probable that the residual discrepancy in the three methods is referable to a lateral motion of the slit itself, due to insufficient symmetry of the slides $AA$ and $BB$ in the above adjustment. This agrees, moreover, with the residual shift observed in the case of parallel rays in §8. The remedy should present no difficulty.

**10. Reflecting plate grating.**—The adjustment of the plane grating if cut on specular metal is nearly identical to the above, except that the collimator is fixed as a whole in front of the grating, either to the slide carrying the standard of the grating, $B$, or else quite in front of the cross slide $AA$, fig. 1 above, so as to give clearance for the to-and-fro motion of the rail, $R$. This admits of measurement of $x$ on both sides of the slit, so that $2x$, the distance apart of the two symmetrical positions for a given spectrum line, is again observed.

**11. Rowland's concave grating.**—For the case of the *concave* grating, the accurate adjustment for symmetrical measurement on *both* sides of the slit is not feasible, because the slit and eyepiece would have to pass through each other. It is possible, however, to find conjugate foci at different distances from the grating in the normal position, which approximately answer the purposes of measurement. Rowland's equation

$$(\cos i/\rho - 1/R)\cos i + (\cos \theta/\rho' - 1/\rho')\cos \theta = 0$$

where $\rho$ and $\rho'$ are the conjugate focal distances for angles of incidence and deviation $i$ and $\theta$, may for $\theta = 0$ be written

$$\frac{1}{\rho/\cos^2 i} - \frac{1}{R/\cos i} = \frac{1}{\rho_0} - \frac{1}{R}$$

where $\rho_0$ is the normal distance of the eyepiece, so that

$$\frac{1}{\rho_0} - \frac{1}{\rho_0'} = \frac{2}{R}$$

If in fig. 4 (page 5) the slit $S$ is put at $\rho' > R$ from the grating $G$ (normal position), the image is at $E$ at the end of $\rho_0$ from $G$, where $\rho_0 < R < \rho'$. If $\rho_0$ be used as a rail instead of $R$ and put at an angle of incidence $i$, for the eyepiece at $E'$ or $E''$, $\rho_0 \cos i > \rho$. But this excess need not be so large as to interfere with adequately sharp focussing.

Table 4 gives an example, in which the difference of $\rho_0$ and $\rho_0'$ in the normal position is even over 1 foot, an excessive amount, as the distance necessary for clearance need not be more than a few inches. The grating has 14,436 lines to the inch and a radius about $R = 191$ cm.

TABLE 4.—Conjugate foci of the concave grating. $R = 191$ cm., 14,436 lines to inch, 5683 lines to cm. $D = .000,176$. $\rho_0 = 166$ cm., $\rho = 198$ cm., $\rho - \rho_0 = 32$ cm. $1/\rho_0 - 1/R = .000,788$, $\theta = 0$, $\sin i = \lambda/D$.

| $i°$ | $\rho$ | $\rho_0 \cos i$ | Diff. | $(\rho/\cos i)^2$ | Fraunhofer lines. | $i$ |
|---|---|---|---|---|---|---|
| | *cm.* | | *cm.* | | | |
| 0° | 166.0 | 166.0 | .0 | 27500 | B | 22° 59′ |
| 5 | 165.3 | 165.3 | .0 | 27500 | C | 21° 54′ |
| 10 | 163.2 | 163.5 | .3 | 27400 | D | 19° 34′ |
| {15 | 159.6 | 160.3 | − .7 | 27300 | E | 17° 26′ |
| {20 | 154.7 | 156.0 | −1.3 | 27100 | F | 16° 02′ |
| 25 | 148.5 | 150.4 | −1.9 | 26800 | G | 14° 10′ |
| 30 | 140.9 | 143.7 | −2.8 | 26500 | .... | .... |
| 35 | 132.2 | 136.0 | −3.8 | 26000 | .... | .... |
| 40 | 122.3 | 127.1 | −4.8 | 25500 | .... | .... |

The greater part of the visible spectrum is thus contained between $i = 15°$ and $i = 20°$. It follows that the excess of $\rho_0 \cos i - \rho$ lies between 7 and 13 mm. Hence the eyepiece may be placed at a mean position corresponding to 10 mm. and give very good definition of the whole spectrum without refocussing, as I found by actual trial. Within 1 cm. the focus is sharp enough for most practical purposes. If the distances $\rho_0$ and $\rho_0'$ are selected so that eyepiece and slit just clear each other the definition is quite sharp.

The diffraction equation is not modified and if $2x$ corresponds to the positions $+i$ and $-i$ for the same spectrum line,

$$2\lambda = (D/R)\,2x$$

It is therefore not necessary to touch the eyepiece and this is contributory to accuracy.

If Rowland's equation is differentiated relatively to $\rho$ and $\rho'$, $-d\rho = \left(\frac{\rho}{\rho_0' \cos i}\right)^2 d\rho_0'$ where the factor $d\rho_0'/\rho_0'^2$ is constant. Hence $-d\rho$ varies as $(\rho/\cos i)^2$, given in the table. If, furthermore, a comparison is made between $d\rho_0$ and $d\rho$ this equation reduces to

$$\sqrt{d\rho_0/d\rho} = (R - \rho_0(1 - \cos i))/R \cos i$$

which becomes unity either for $i = 0$ or for $\rho_0 = R$ (Rowland's case).

**12. Summary.**—By using two slides symmetrically normal to each other and observing on both sides of the point of interference, it is shown that many of the errors are eliminated by the symmetrical adjustments in question. The slide carrying the grating may be provided with a focussing lens in front or again behind it, if the means are at hand for actuating the slit which is not sharply in focus on the plane of the eyepiece carried by a second slide throughout the spectrum at a given time. It is thus best to use both lenses conjointly, the latter as a collimator and the former as an objective of the telescope in connection with the eyepiece. It is shown that a centimeter scale parallel to the eyepiece slide with a vernier reading to millimeters is sufficient to measure the wave-lengths of light to few Angström units, while the wave-lengths are throughout strictly proportional to the displacements along the scale. The errors of the three available methods and their counterparts are discussed in detail. The method is applicable both to the transparent and the reflecting grating.

It is furthermore shown that, in case of Rowland's concave grating, observation may be made symmetrically on both sides of the slit, by providing for reasonable clearance of slit and eyepiece passing across each other, although one conjugate focal distance is now not quite the projection of the other.

# CHAPTER II.

## THE INTERFERENCE OF THE REFLECTED-DIFFRACTED AND THE DIFFRACTED-REFLECTED RAYS OF A PLANE TRANSPARENT GRATING, AND ON AN INTERFEROMETER. By C. Barus and M. Barus.

**13. Introductory.**—If parallel light, falling on the front face of a transparent plane grating, is observed through a telescope after reflection from a rear parallel face (see fig. 5), the spectrum is frequently found to be intersected by strong, vertical interference bands. Almost any type of grating will suffice, including the admirable replicas now available, like those of Mr. Ives. In the latter case one would be inclined to refer the phenomenon to the film and give it no further consideration. On closer inspection, how-

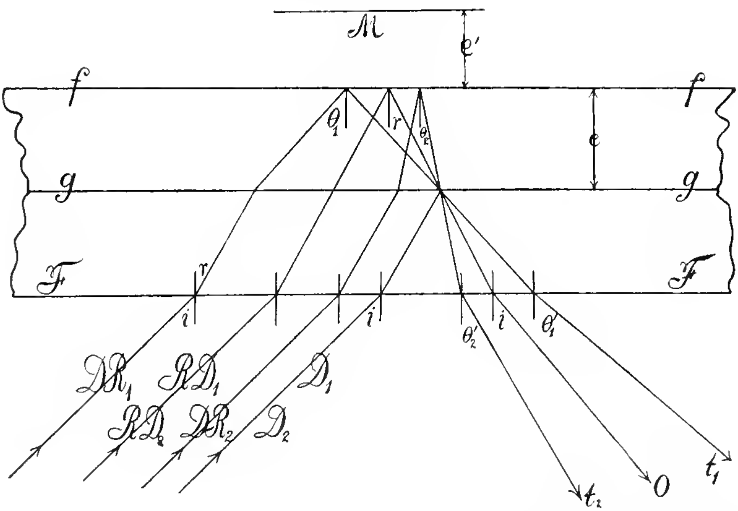


FIG. 5.—Showing the three incident rays interfering in the diffracted ray $t_1$, ($\theta_2' > i$), and the three rays interfering similarly in the ray $t_2$, ($\theta_1' < i$). *DR* is first diffracted and then reflected, and the reverse is true for *RD*. *D* is diffracted only.

ever, it appears that the strongest fringes certainly have a different origin and depend essentially on the reflecting face behind the grating. If, for instance, this face is blurred by attaching a piece of rough, wet paper, or by pasting the face of a prism upon it with water, so as to remove most of the reflected light, the fringes all but disappear. If a metal mirror is forced against the rear glass face, whereby a half wave-length is lost at the mirror but not at the glass face in contact, the fringes are impaired, making a rather interesting experiment. With homogeneous light the fringes of the film itself appear to the naked eye, as they are usually very large by comparison.

Granting that the fringes in question depend upon the reflecting surface behind the grating, they must move if the distance between them is varied. Consequently a phenomenon so easily produced and controlled is of much greater interest in relation to micrometric measurements than at first appears and we have for this reason given it detailed treatment. It has the great advantage of not needing monochromatic light, of being applicable for any wave-length whatever, and admitting of the measurement of horizontal angles. In chapter 5 it will be shown that these interferences may also be produced by Michelson's or by Jamin's apparatus.

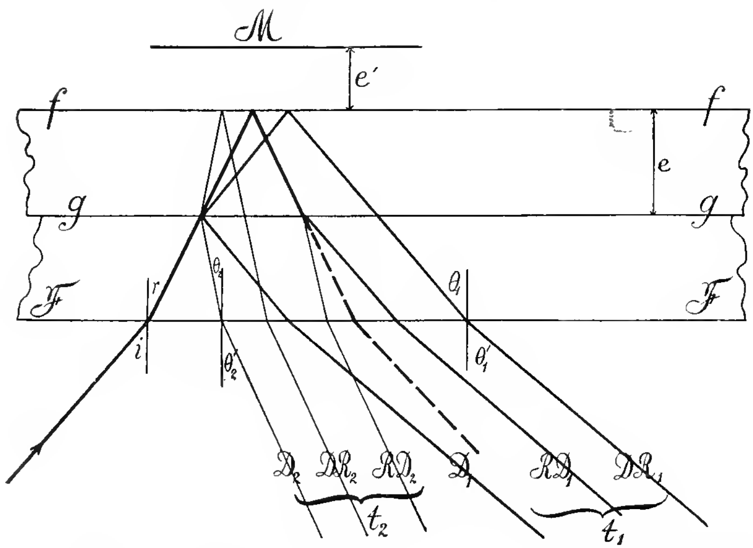


FIG. 6.—Showing corresponding triplets of diffracted rays for a single incident ray, and each of the cases $\theta_1' > i$ and $\theta_2' < i$ of fig. 5.

When the phenomenon as a whole is carefully studied it is found to be multiple in character. In each order of spectrum there are different groups of fringes of different angular sizes and usually in very different focal planes. Some of these are associated with parallel light, others with divergent or convergent light, so that a telescope is essential to bring out the successive groups in their entirety. At any deviation the diffracted light is necessarily monochromatic, but the fringes need not and rarely do appear in focus with the solar spectrum. If the slit of the spectroscope is purposely slightly inclined to the lines of the grating, certain of the fringes may appear inclined in one way and others in the opposite way, producing a cross pattern like a pantograph. The reason for this appears in the equations.

In any case the final evidence is given when the reflecting face behind the grating is movable parallel to it. The interferometer so obtained is subject to the equation (air space $e$, wave-length $\lambda$, angle of incidence $i$, of diffraction $\theta'$), $\delta e = \lambda/2(\cos\theta' - \cos i)$, and is therefore less unique as an absolute instrument than Michelson's classic apparatus or the device of Fabry and Perot. Its sensitiveness per fringe, $\delta e$, depends essentially upon the angle of incidence and diffraction and it admits of but 1 cm. (about) of air-space between grating face and mirror before the fringes become too fine to be available. But on the other hand it does not require monochromatic light (a Welsbach burner suffices), it does not require optical plate glass, it is sufficient to use but a square cm. of grating film, and it admits of very easy manipulation, for painstaking adjustments as to normality, etc., are superfluous. In fact it is only necessary to put the sodium lines in the spectrum reflected from the grating and from the mirror into coincidence

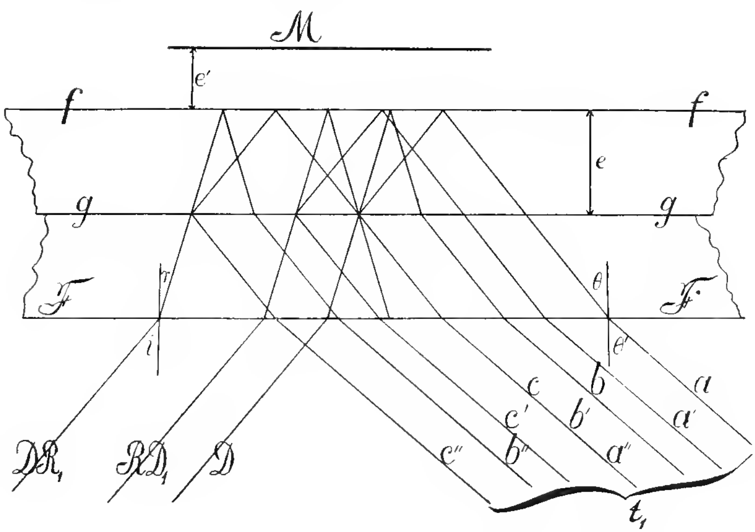


FIG. 7.—Superposition of the cases of figs. 5 and 6 for $\theta' > i$.

both horizontally and vertically with the usual three adjustment screws on grating and mirror. Naturally sunlight is here desirable. Thereupon the fringes will usually appear and may be sharply adjusted upon a second trial at once.

When the air-space is small, coarse and fine fringes (fluted fringes) are simultaneously in focus, one of which may be used as a coarse adjustment on the other. Finally, the sensitiveness per fringe to be obtained is easily a length of one-half wave-length in the fine fringes and one wave-length in the coarse fringes, though the latter may also be increased almost to the limit of the former. The fine fringes compatibly with their greater sensitiveness vanish within about a millimeter. Their occurrence with the coarse fringes makes it possible to investigate sudden displacements within the latter.

TABLE 5.—Interferences. Grating between plates of glass each 0.48 cm. thick. Additional rear plate (mirror) 0.29 cm. thick. Index of refraction of glass $\mu = 1.527$.

| Side. | Order. | Color. | Rays. | $i$ | Mean $\theta'$ | Observed $\partial\theta'$ Minutes. | Computed $\partial\theta'$ Minutes. | Remarks. |
|---|---|---|---|---|---|---|---|---|
| | | | | ° | ° ′ | | | |
| $\theta > r$ | | | | | | | | |
| $r = 0$ | 1 | C | Convergent* | 0 | 24 8 | 1.87 | 1.81 | About double divergence, but not clear. |
| $\theta = 15° 49'$ | 2 | | | | | | | |
| $r > \theta$ | 1 | D to E | Less convergent | 45 | 21 1 | 1.80 | 1.70 | Strong. Total. |
| $r = 27° 35'$ | 1 | Do. | Parallel | 45 | 21 21 | .35 | ... | Estimated.† |
| $\theta = 13° 35'$ | 1 | Do. | Divergent | 45 | 21 32 | .70 | ... | Estimated.† |
| | 1 | Do. | More divergent | 45 | 22 40 | .87 | .... | |
| $r > 0$ | 2 | Do. | Convergent | 45 | 31 | 3.32 | .. | Clear, but faint. |
| | 2 | Do. | Convergent | 45 | .... | .8 | . | Very fine and close. |
| | 2 | Do. | Parallel | 45 | 31 | 1.20 | ... | |
| | 2 | Do. | Divergent | 45 | .... | .... | ... | Not clear. $\partial\theta' = 2.0'$? |
| | 2 | Do. | Very divergent | 45 | .... | .... | ... | Not clear. $\partial\theta' = 3.0'$? |
| $r < \theta$ | 1 | D to E | Very divergent | 22.5 | 1 30 | 4.7 | .... | Faint, but certain. |
| $r = 14° 31'$ | 1 | Do. | Divergent | 22.5 | .... | ... | .... | Faint. $\partial\theta' = 2'$? |
| $\theta = 1° 23'$ | 1 | Do. | Nearly parallel | 22.5 | .... | ... | .... | Faint. $\partial\theta' = 1.5'$? |
| | 1 | Do. | Parallel | 22.5 | .... | ... | .... | Fine, close, and strong |
| | 1 | Do. | Convergent | 22.5 | 2 6 | 1.85 | 1.84 | Strong. Total. |
| Interferometer: | | | | | | | | |
| | 1 | D to E | .............. | 22.5 | ... | 1.83 | 1.84 | $e = .48$ cm. Total. |
| | 1 | Do. | .............. | 22.5 | .... | 1.13 | 1.15 | $e' = .77$ cm. Total. |

* Color not definite, only end of red spectrum seen.

† Lines strong, but too fine and close together.

**14. Observations.**—The following observations were made merely to corroborate the equations used. The general character of the results will become clear on consulting the preceding abbreviated table chosen at random from many similar data. An Ives replica grating with 15,000 lines to the inch (film between plates of glass .46 cm. thick) was mounted as usual on a spectrometer admitting of an angular measurement within one minute of arc. Parallel light fell on the grating, fig. 5, *gg* (see p. 13), under different angles of incidence, $i$, and the spectrum lines were observed by reflection (after reflection from *gg* and the rear face *ff*) at an angle of diffraction $\theta'$ in air, both in the first and second order of spectra, and so far as possible on both sides of the directly reflected beam. In view of the front plate, the angle $i$ corresponds to an angle of refraction $r$, within the glass and the angle $\theta'$ similarly to an angle of diffraction $\theta$, respectively. Hence $r > \theta_2$ or $\theta_1 < r$ denote the sides of the ordinary ray on which observation is made. As a rule these were as nearly as possible in the region of the $D$ line passing toward $E$. Finally $\delta\theta$ denotes the angle between two consecutive dark fringes, observed and computed as specified. Similarly $\delta e$ will be reserved for changes of thickness $e$ of the glass and $\delta e'$ for changes of the air space in case of an auxiliary mirror $M$.

For $i = 0°$ the number of groups of lines was a single set in each order; but only the end of the spectrum could be seen. Measurements refer (about) to the $C$ line. For $i = 45°$ several groups were too close together, or too faint for measurement, and the same is true for $i = 22.5°$. An estimate of divergence is all that could be attempted on the given spectrometer. The case $\theta_1 > r$ was usually not available, but for $i = 22.5°$ two sets were found in the first order, one being the normal set. The fringes in all cases decrease in size from red to violet, but less rapidly than wave-length.

Whether they are convergent or divergent for a given set of fringes, as for instance for the strong set, depends on the position of the grating. Thus the divergent rays become convergent when the grating is rotated 180° about its normal. It is therefore definitely wedge-shaped. In fact when the auxiliary mirror $M$ is used, the fringes may be put anywhere, either in front of or behind the principal focal plane, by suitably inclining the mirror.

**15. Equations.**—If we suppose the film of the grating *gg* to be sandwiched in between plates of glass each of thickness $e$, it will be seen that triplicate rays pass in the direction $t_1$, $(\theta_1' > i)$ or of $t_2$, $(\theta_2' < i)$, which will necessarily produce interference either partial or total. With respect to $t_1$, the only light received comes either from $D_1$ by direct diffraction at *gg*, or from $RD_1$, by reflection from the lower face *ff*, and thereafter by diffraction at *gg*; or from $DR_1$, by diffraction at *gg* and reflection at *ff*. Similarly the light along $t_2$ comes in like manner either from $D_2$ or $DR_2$ or $RD_2$. With regard to the angles of incidence and refraction or of diffraction within the glass or outside of it, we have the equations for the first and second order of spectra ($D$ being the grating space).

$$\sin i_1 = \mu \sin r_1 \quad (1)$$
$$\sin \theta_1' = \mu \sin \theta_1 \quad (2)$$
$$\sin \theta_2' = \mu \sin \theta_2 \quad (3)$$
$$\sin r - \sin \theta_2 = \lambda/D\mu, \text{ or} = 2\lambda/D\mu \quad (4)$$
$$\sin \theta_1 - \sin r = \lambda/D\mu, \text{ or} = 2\lambda/D\mu \quad (5)$$
$$\sin i - \sin \theta_2' = \lambda/D, \text{ etc.} \quad (4')$$
$$\sin \theta_1' - \sin i = \lambda/D, \text{ etc.} \quad (5')$$

where $\mu$ is the index of refraction of the glass, found to be equal to 1.5265 for sodium light, by breaking off a small corner of the glass of the grating and using Kohlrausch's total reflectometer.

Furthermore, for the occurrence of interference along $t_1$ we shall have, for the case of the three rays in question, respectively combined in pairs, if the wave fronts be taken in the glass plate $FFgg$

$$n\lambda = 2e\mu \cos r \quad (6'')$$
$$n\lambda = 2e\mu(1 - \sin \theta_1 \sin r)/\cos \theta_1 \quad (7'')$$
$$n\lambda = 2e\mu(1 - \cos (\theta_1 - r))/\cos \theta_1 \quad (8'')$$

where $n$ is the order of interference and a whole number, $e$ the thickness of the lower glass plate, as may be found from a consideration of wave fronts and need not be deduced here. It will be seen that, whereas equations 6 and 7 present cases of partial interference, equation 8, which is virtually the difference of 6 and 7, should be a case of total interference, giving strong fringes and possibly useful for interferometry.

Again for $t_2$ the equations will be similar if corresponding wave fronts be taken in the glass plate $FFgg$

$$n\lambda = 2e\mu \cos r \quad (6')$$
$$n\lambda = 2e\mu(1 - \sin \theta_2 \sin r)/\cos \theta_2 \quad (7')$$
$$n\lambda = 2e\mu(1 - \cos (r - \theta_2))/\cos \theta_2 \quad (8')$$

the same as in the preceding case when $\theta_1$ is replaced by $\theta_2$ and $\theta_1 - r$ by $r - \theta_2$. To this extent there is no essential difference between the cases. Therefore $\theta$ may be used indiscriminately for either.

If, however, the wave fronts be taken in the glass plate $ffgg$ the equations become

$$n\lambda = 2e\mu \cos r \quad (6)$$
$$n\lambda = 2e\mu \cos \theta_1 \quad (7)$$
$$n\lambda = 2e\mu (\cos r - \cos \theta_1) \quad (8)$$

with three other corresponding forms for $\theta < r$, as before. The latter are the true equations and equation 8 is the case of total interference.

These circumstances are at first quite puzzling, but they are due to the fact that in the cases 6′, 7′, 8′, 6″, 7″, 8″, the wave fronts taken correspond to the refracted ray only, whereas the diffracted rays subsequently undergo sudden changes of deviation on leaving $gg$. We have nevertheless carried both groups of equations 6′ to 8′ and 6 to 8 in mind, though the latter are alone certain of application.

For an air-space between $gg$ and $M$ the equations would be

$$n\lambda = 2e \cos i \qquad n\lambda = 2e \cos \theta' \qquad n\lambda = 2e\,(\cos \theta' - \cos i),\ \text{etc.}$$

**16. Differential equations.**—The quantity measured on the spectrometer is essentially angular and preferably $d\theta'/dn$, the angular distance apart of the fringes, in radians. Later we shall measure $\delta e$ or the linear displacement of the parallel faces per fringe. In any measurement, however, we meet with embarrassment, inasmuch as $n$, $\lambda$, $\mu$, $r$, $\theta$, $\theta'$, are all variable. The angle $i$ and the thickness $e$ and the grating space $D$ are alone given. Among these, the variation of $r$ with $\mu$ and $\lambda$ must be found by experiment. Fortunately, in case of the interferometer all these variables are eliminated and $e$ alone changes, subject to a given $i$ and $\theta'$. The $\mu$ used need not be known. (See paragraph 19.)

For the present purpose, as the variation of $\mu$ enters only as a correction, we have been satisfied with the usual results in physical tables.* If from the $C$ to the $D$ line

$$(d\mu/\mu)/(d\lambda/\lambda) = -.016$$

and from the $B$ to the $C$ line, $= -.013$, we may write

$$-\frac{d\mu}{\mu} = .015\frac{d\lambda}{\lambda}$$

and therefore

$$d\left(\frac{\lambda}{\mu}\right) = 1.015\frac{d\lambda}{\mu} \tag{9}$$

We shall write $a = .015$, $b = 1 + a$.

The case $\theta > r$ in the present paper is not of much experimental interest, and may be omitted here. For the case of $r > \theta$ we shall have successively and for the total interferences $RD$, $DR$, equation 8,

$$-\frac{d\lambda}{d\mu} = \frac{\lambda \cos \theta}{\sin r - b \sin \theta}\frac{d\theta}{dn} \tag{11}$$

$$-\frac{dr}{dn} = a\frac{\tan r \cos \theta}{\sin r - b \sin \theta}\frac{d\theta}{dn} \tag{12}$$

$$\frac{d\mu}{dn} = \frac{a\mu \cos \theta}{\sin r - b \sin \theta}\frac{d\theta}{dn} \tag{13}$$

$$\frac{d\theta'}{dn} = \frac{\mu \cos \theta(\sin r - \sin \theta)}{\cos \theta'(\sin r - b \sin \theta)}\frac{d\theta}{dn} \tag{14}$$

* See Kohlrausch's Leitfaden, 11th edition, 1910, p. 712, light crown glass being taken.

and finally corresponding to equations 6, 7, 8,

$$\frac{d\theta'}{dn}=\frac{\cos\theta}{2e\cos\theta'}\;\frac{\lambda(\sin r-\sin\theta)}{b-\sin r\sin\theta} \tag{15}$$

$$\frac{d\theta'}{dn}=\frac{\cos\theta}{2e\cos\theta'}\;\frac{\lambda(\sin r-\sin\theta)}{b\cos r\cos\theta+a\sin r\tan r\cos\theta} \tag{16}$$

$$\frac{d\theta'}{dn}=\frac{\cos\theta}{2e\cos\theta'}\;\frac{\lambda(\sin r-\sin\theta)}{b(1-\cos(r-\theta))+a\sin r\sin\theta(1-\cot\theta\tan r)} \tag{17}$$

the last term in the denominator being corrective. Here $d\theta'/dn$ is the observed angular deviation of two consecutive fringes, so that

$$\frac{dn}{d\theta_1'}-\frac{dn}{d\theta_2'}=\frac{dn}{d\theta_3'}$$

The equation corresponding to the incorrect equation 8′ would have been

$$\frac{d\theta'}{dn}=\frac{\cos\theta}{2e\cos\theta'}$$

$$\frac{\lambda\cos^2\theta(\sin r-\sin\theta)}{b\cos^2\theta(1-\cos(r-\theta))-(\sin r-\sin\theta)(\sin r-b\sin\theta)-a\tan r\cos^2\theta\sin(r-\theta)}$$

**17. Normal incidence or diffraction, etc.**—For the case of normal incidence $i=r=0$, the equations corresponding to 6, 7, and 8 take a simplified form and are respectively

$$-\frac{d\theta_0'}{dn}=\frac{\lambda\sin\theta\cos\theta}{2be\cos\theta'} \tag{15'}$$

$$-\frac{d\theta_0'}{dn}=\frac{\lambda\sin\theta}{2be\cos\theta'} \tag{16'}$$

$$-\frac{d\theta_0'}{dn}=\frac{\cos\theta}{2be\cos\theta'}\;\frac{\lambda\sin\theta}{1-\cos\theta} \tag{18'}$$

If $\theta'=\theta=0$, for normal diffraction, which is particularly useful in Rowland's adjustments as well as on the spectrometer

$$-\left[\frac{d\theta'}{dn}\right]_{\theta=0}=\frac{\lambda}{2e}\;\frac{\sin r}{b(1-\cos r)-a\sin r\tan r}$$

for the case of total interference corresponding to equations 8 and 17. If $i=-\theta'$ or $r=-\theta$

$$\left[\frac{d\theta'}{dn}\right]_{r=-\theta}=\frac{\lambda}{2e}\;\frac{1}{\tan\theta\cos\theta'}$$

**18. Comparison of the equations of total interference with observation.**—The partial interferences corresponding to equations 6 and 7 are usually too fine to be seen unless $e$ is very small. They amount in cases of equations 15 and 16 for $e=.48$ cm. to the following small angles

| | (15) | (16) |
|---|---|---|
| $i=0^\circ$ | $d\theta'/dn=.060'$ | $d\theta'/dn=.062'$ |
| $22.5^\circ$ | $.048'$ | $.050'$ |
| $45^\circ$ | $.057'$ | $.058'$ |

usually less than four seconds of arc and are therefore lost. The origin of the fine interferences actually seen in the table is thus still open to surmise. With small $e$ and the interferometer they are obvious.

The total interferences as computed in the above table agree with the observations to much within 0.1 minute of arc and these are experimental errors; particularly so as it was not possible to use both verniers of the spectrometer. The interesting feature of the experiment and calculation is this, that $\delta\theta'$ has about the same value for all incidences $i$ from 0° to 45° and even beyond. The equations do not show this at once, owing to the entrance of $\mu$ and $r$. But apart from $a$ and $b$ equation 17 is nearly

$$\frac{d\theta}{dn}=\frac{\lambda}{2e\mu}\;\frac{\lambda/D}{1-\cos(r-\theta)} \qquad (19)$$

which is independent of $r$ to the extent in which $\cos(r-\theta)$ is constant. The dependence of $d\theta'/dn$ on wave-length is borne out. (See paragraph 19.) Finally, $d\theta'/dn$ is independent of $\mu$ except as it occurs in $a$ and $b$.

If the glass plate *ffgg* is removed and a mirror $M$ used, as in the interferometer, the fringes may be enormously enlarged by decreasing $e$ and the measurements made with any degree of accuracy; but such measurements were originally impracticable and have little further interest in this place since the interferometer itself is tested in the next chapter.

**19. Interferometer.**—The final test of the above equation is given by the last part of the table for different thicknesses of glass, $e=.48$ and $e=.77$ cm. The results are in perfect accord.

These data suffice to state the outlook for the interferometer. In this case $n$ and $e$ are the only variables, so that equation 8 becomes

$$\delta e=\lambda/2\mu(\cos\theta-\cos r) \qquad (20')$$

where $\delta e$ is the thickness of glass corresponding to the passage of one fringe across the cross-hairs of the telescope or a definite spectrum line.

If instead of glass in the grating above, an air-space intervenes between the film of the grating and the auxiliary mirror $M$, fig. 5, the equation reduces to

$$\delta e=\frac{\lambda}{2(\cos\theta'-\cos i)}=\frac{\lambda}{2\left(\sqrt{1-(\sin i-\lambda/D)^2}-\cos i\right)} \qquad (20)$$

where $i$ and $\theta'$ are the angles of incidence and diffraction in air.

These equations 20 embody a curious circumstance. Inasmuch as $\theta$ and $\theta'$ change as $i$ increases from 0° to 90° from negative to positive values at about $i=13°$ and $i=20°$, respectively, the denominator of either equation 20 will pass through zero (for air at about $i=10°$). Hence at this value of $i$ the motion of the mirror $M$ produces no $e$ effect (stationary fringes), while on either side of it the fringes travel in opposite directions in the telescope when $e$ changes by the same amount. In the negative case the sensitiveness for air-spaces passes from $\delta e=-.000\,489$ to $\delta e=-\infty$, per fringe. In the positive case from $\delta e = +\infty$ to $\delta e = .000\ 039$, per fringe or to a limit of about a half wave-length in case of 15,000 lines to the inch. This limiting sensitiveness may be regarded as practically reached even at $i = 40°$ where $\delta e = .000\ 155$ cm. per fringe and an angle of about $i = 45°$ is most convenient in practice.

In addition to the large fringes the fine set appears when $e$ is small or not more than a few tenths of a millimeter. The sensitiveness of these is naturally much more marked. In the two cases

$$\delta e = \lambda/2 \cos i \qquad (20')$$

$$\delta e = \lambda/2 \cos \theta' \qquad (20'')$$

so that nearly $\lambda/2$ per fringe is easily attained, but the available thickness of air-space within which they are visible is decreased.

At $i = 20°$ about, and in case of an air-space $\theta'$ is nearly $0°$ We suggested above that these fine fringes may be used as a fine adjustment in connection with the large fringes, on which they are superimposed. In appearance these large fluted fringes are exceedingly beautiful. The fine fringes have the limiting sensitiveness of the coarse fringes, *i.e.*, the cases for $i = 90°$ or $\theta'$ equal to maximum value. In different focal planes both sets of fine fringes may be seen separately for small $e$ (air wedge).

Equation 20 shows that for smaller grating spaces $D$, and consequently also in the second order of spectra there must be greater sensitiveness, *caet. par.*; but as a rule we have not found these fringes as sharp and useful as those in the first order.

The limiting sensitiveness per fringe, however, follows a very curious rule. If in equation 20 we put $i = 90°$,

$$2\delta e = \sqrt{\lambda D/(2 - \lambda/D)} = \lambda/\sqrt{r(2 - r)} \text{ in the first order}$$

if $r = \lambda/D$, and

$$2\delta e = \sqrt{\lambda D/4(1 - \lambda/D)} = \lambda/2\sqrt{r(1 - r)} \text{ in the second order}$$

$D$ is the grating space. Both equations have a minimum, $\delta e = \lambda/2$, at $\lambda/D = 1$ in the first order and $\lambda/D = .5$ in the second order, beyond which it would be disadvantageous to decrease the grating space. These minimum conditions are as good as reached even when $D$ corresponds to 15,000 lines to the inch, as above, where roughly $10^6 \delta e = 38$ cm. in the first order and $10^6 \delta e = 33$ cm. in the second order.

All the conditions discussed above are summarized in fig. 8 and fig. 9 for the first and second orders of spectrum.

To view the stationary fringes of the first order was not practicable, since they occurred for $i = 10°$, whereas the telescopes were in contact at about $20°$. In the second order of spectra they may be approached more nearly as they occur when $i$ is roughly $20°$. If the distance $e$ is made small enough, so that the three cases of equations 20, $20'$, $20''$, are visible, the appearance is very peculiar. The fringes of equation 20 are very slow-moving. They are intersected by the small fringes of equation 20′, producing the fluted pattern already discussed. Over all travel the rapidly moving fringes of equation 20″, producing a kind of alternation or flickering which it is very difficult to analyze or interpret until $e$ is very small, when all three sets are broad and easily recognized. Sunlight should be used. Nothing like these alternating fringes was seen in the first order, but we used a film grating only.

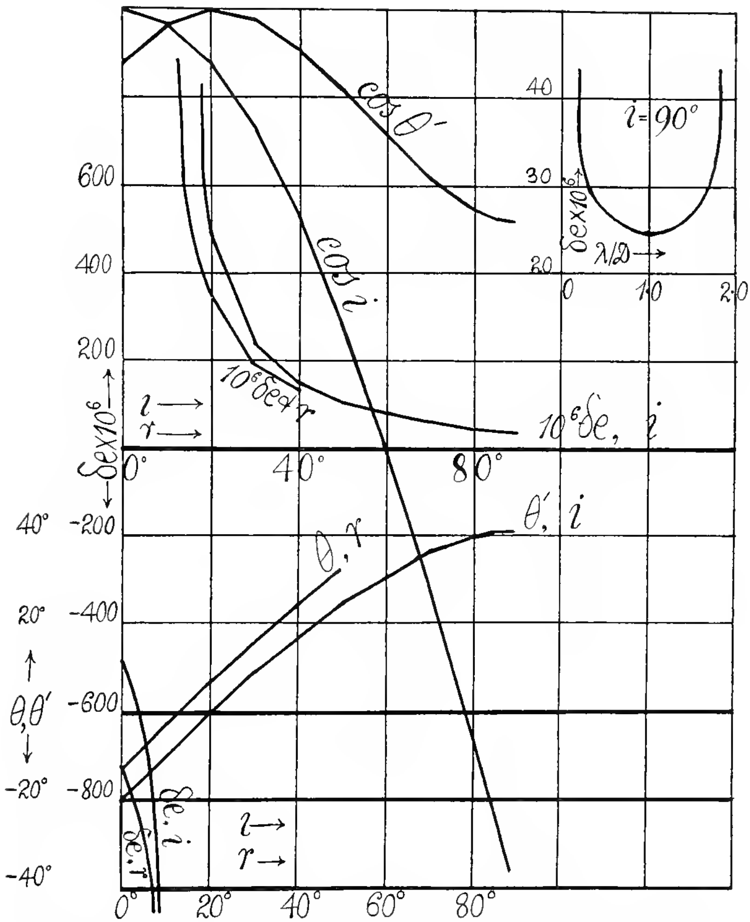


FIG. 8.—Charts showing dependence of $\theta$ on $r$, $\theta'$ on $i$, cos $\theta'$ and cos $i$ on $i$, $\delta e$ on $r$ and $\delta e$ on $i$, $\delta e$ on $\lambda/D$ for the first order of spectrum.

The above equation shows finally that $\delta e$ is not exactly proportional to wave-length, though the former decreases with the latter, as shown above.

The three equations 20 indicate finally that for $i > \theta'$ all fringes travel in the same direction with increasing $e$; whereas if $\theta' > i$, the set corresponding to equation 20 travel in a direction opposite to that of the sets 20′ and 20″

This is strikingly borne out by making the experiment for $\theta > i$ with a small angle $i$, both in the first and second order.

Table 6 contains a few data obtained by carrying the mirror on a Fraunhofer micrometer, reading to .0001 cm., toward a stationary grating film.

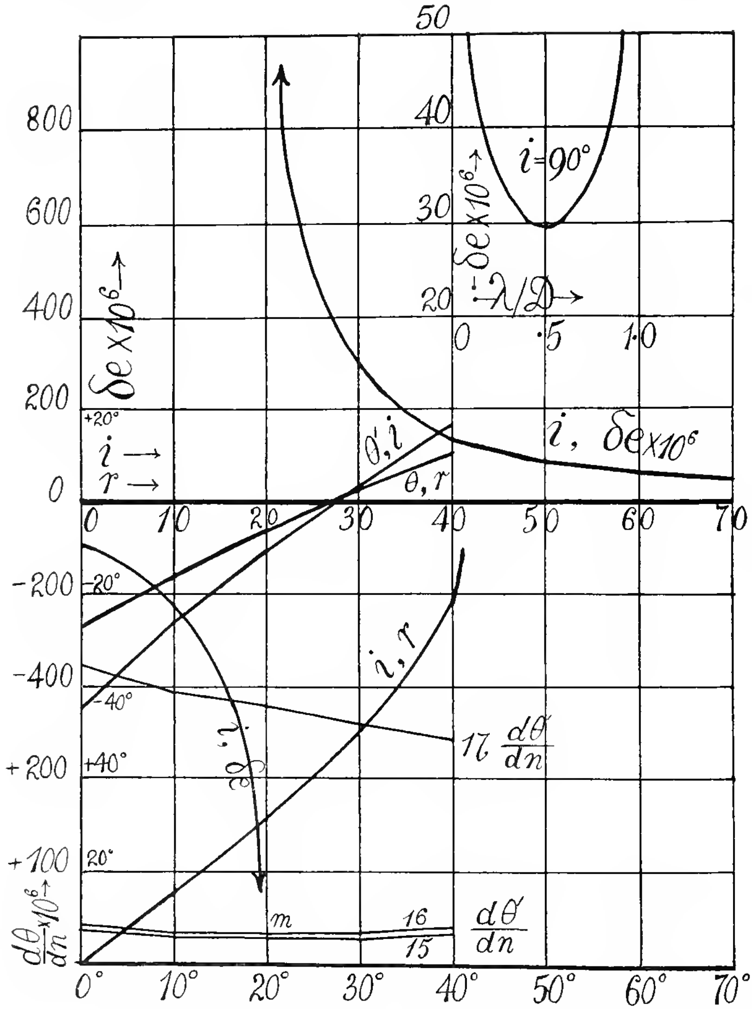


Fig. 9.—Similar data to those of fig. 8, for the second order of spectrum. In addition, $d\theta'/dn$ is shown as given by equations 15, 16, 17.

Observations were made in the region of the $D$ lines. The grating was originally between plates of glass $e = .48$ cm. thick. Finally the plate between grating and mirror was removed, the whole distance now being an air-space. This has no effect on $\delta e$, but $e$ may then be reduced to zero and the fringes enlarged.

These data merely test the equations, as no special pains were taken for accurate measurement, which neither the micrometer screw nor the special adjustments warranted. Usually the micrometer equivalent of 50 fringes was observed on the screw. The maximum distance $e$ between grating and mirror was .48 cm. of glass and .25 cm. of air conjointly, or within 1 cm. In case of fine fringes mere pressure on table or screw impaired the adjustment. Moreover these fine fringes run through the shadow of the coarse fringes, and their size in consecutive spaces between the latter seems to vary periodically as if they alternated between the two equations 15 and 16.

TABLE 6.—Interferometer measurements. Replica grating. Air-space, often in addition to glass space, $e=.46$ cm.

| $i$ | $\theta'$ | Coarse fringes. Air-space.* | Coarse fringes. Observed. $\delta e\times 10^6$ | Coarse fringes. Computed. $\delta e\times 10^6$ | Fine fringes. Air-space. | Fine fringes. Observed. $\delta e\times 10^6$ | Fine fringes. Computed. $\delta e\times 10^6$ |
|---|---|---|---|---|---|---|---|
| | | *cm.* | *cm.* | *cm.* | *cm.* | *cm.* | *cm.* |
| 22° 30′ | 2° 6′ | .02 to .33 | 390 | Co., 391 | .... | .... | .... |
| 45 0 | 21 1 | .03 | 131 | 130 | .... | .... | .... |
| 67 30 | 35 1 | .03 | 72 | 68 | .... | .... | .... |
| 25 0 | 4 7 | .... | 322 | 324 | .... | .... | .... |
| 30 2 | 8 37 | .013 to .250 | 241 | 240 | .... | .... | .... |
| Glass removed between mirror and grating. | | | | | | | |
| 22° 25′ | 1° 40′ | .013 to .054 | 387 | 392 | .006 to .025 | 34 | 32, 30 |
| 45 0 | 20 49 | .032 to .064 | 129 | 130 | .000 to .007 | 33 | 42, 32 |

* Approximate; contact endangering adjustment.

**20. Secondary interferences.**—We come now to consider the minor interferences which are either weaker, finer, or more diffuse than the strong forms discussed. In the interpretation of these we have not met with success, but some reference to them is essential. We assume that after two reflections the fringes can no longer be seen.

In fig. 6 if there is light reinforcement passing in any direction $t_1$ or $t_2$; then each incident ray $I$, at an angle $i$ with the normal $n$, will after refraction be represented by the six rays $D_1\ RD_1\ DR_1\ (\theta_1>r)$, $D_2\ DR_2\ RD_2\ (\theta_2<r)$, as shown in the figure, under a notation similar to the preceding case. If these rays are brought to a focus by a telescope there must be interferences between pairs of which the fringes of $D$, $RD$, and $D$, $DR$, will usually be too fine to be visible, whereas $RD$, and $DR$, will be large enough to be seen.

As the lines are not quite sharp, measurement is difficult and no other fringes were therefore computed, and we have not thus far been at pains to discover a reason for the large fringes in table 1, either in the first order ($i=22.5°$, $\delta\theta'=4.7'$) or in the second order ($i=45°$, $\delta\theta'=3.3'$).

**21. Summary of secondary interferences.**—The possible partial interferences are naturally numerous. If we superimpose the case of fig. 5 on fig. 6 and draw all the rays of the first reflection for $\theta > r$ only (to avoid complications), *i. e.*, for a single direction, it will be seen that nine rays are included, of which $a, b, c, a', b', c', a'', b'', c''$, come from a single incident ray each. Thus we can assemble these interferences from a determinant like

$$\begin{matrix} a & b & c \\ a' & b' & c' \\ a'' & b'' & c'' \end{matrix}$$

and there should be 18 cases. Most of these are identical in path difference, but they have not led us to any satisfactory identification. They may therefore be omitted here.

Other difficulties enter. Fringes which may be invisible if observed for the glass plate may be visible if arising in the collodion film, as this is very thin. Possibly some of the finer lines may arise in this way, but not probably.

The tendency of certain groups of interferences to travel in opposed directions with rotation of the slit has suggested to us the possible occurrence of zone-plate action, where there would be multiple foci. But we have not succeeded in establishing coincidences either for the virtual or real foci in such a case. Moreover this opposition in motion has already been accounted for in paragraph 19.

**22. Convergent and divergent rays.**—What finally characterizes the above groups of interferences is the difference in position of their focal planes. They rarely coincide with the spectrum (parallel rays) and hence do not always destroy it. If present with the spectrum the latter is wholly wiped out. If the strong fringes are convergent for a given adjustment of grating they become divergent when the grating is rotated 180° about its normal. Hence the plates of glass are sharply wedge-shaped and to these differences the location of focal planes is to be referred.

In addition to this the three regular reflections are not in the same focus which shows the surfaces (collodium film) to be slightly curved. The above experiments succeed best when two of the reflections are yellowish, which probably means that the grating face is from the observer.

Suppose the remote glass face makes an angle $dr/2$ with the surface of the grating. Then the $DR$ ray of the strong interferences has its angle incremented by $d\theta = dr$, whereas the $RD$ ray receives an increment of but $d\theta = \frac{\cos r}{\cos \theta} dr$. Hence if the $DR$ and $RD$ rays were parallel for parallel surfaces they would be at an angle corresponding to

$$\frac{d\theta - dr}{dr} = \frac{\cos r - \cos \theta}{\cos \theta} \tag{21}$$

where $dr/2$ is the angle of the wedge. Thus for the partial case of single incidence, fig. 6, $d\theta > dr$ if $\theta > r$, or the issuing rays would converge; and $d\theta < dr$ and $r > \theta$, or the issuing rays would diverge. If $DR$ is negative the opposite conditions will hold, since $dr$ and $d\theta$ change signs together. For the case of triple incidence, fig. 5, there will be similar relations with less liability to convergence. The interferences are further modified by the change of thickness of glass or the variable $e$ implied.

Fig. 7 shows that rays all but parallel will cross each other in front (convergent) or behind (divergent) the grating, depending on their mutual lateral positions. As a ray moves from the right to the left of the normal, the phenomenon may change from divergence to convergence and vice versa.

**23. Measurement of small horizontal angles.**—These relations are very well brought out by the interferometer, in which the mirror $M$ may be inclined at pleasure. If small values of deviation only are in question, this instrument becomes a means of measuring small horizontal angles $\gamma$ between mirror and grating as these involve less change of focus. In fact if $h$ is the vertical height of the illumination at the mirror $M$ and the corresponding obliquity of fringes is equivalent to an excess of $N$ fringes crossing the bottom of the cross-hairs as compared with the top for a wave-length $\lambda$, $\gamma = N\delta e/h$; or

$$\gamma = \frac{N\lambda}{2h\ (\cos\theta' - \cos i)}$$

The question next at issue is thus the value of $h$. It will be noticed that if parallel rays fall upon the slit, they will be brought to a focus by the collimator objective first, and thereafter by the telescope objective, placed at a diametral distance $D$ beyond it. Then if $S$ is the vertical length of slit used, and $f_c$ and $f_t$ the focal lengths of the two objectives, respectively, it follows that the length $h = S$ is virtually illuminated. Hence,

$$\gamma = \frac{N\lambda}{2S\ (\cos\theta' - \cos i)} \qquad (22)$$

For since the angle $\gamma$, or a ratio, is in question, $N\delta e/h$ is constant and it makes no difference where the mirror $M$ may be placed, *i.e.*, how great the absolute vertical height of the illumination $h$ may be.

In case of this method (parallel light impinging on the slit) the illumination at each point of the image is received from but a single point (nearly) of the mirror, whereas if the light falling on the slit is convergent, the whole vertical extent of the mirror illumination contributes to each point of the image in the ocular. Hence in the latter case the fringes are only sharp when $M$ and the grating are rigorously parallel, and they soon become blurred when this is increasingly less true. The same observation also accounts for the greater difficulty in adjustment when lamp-light is used. In any case, equation 22 furnishes $N/S$. $N$ may be obtained with an ocular micrometer.

In the interest of greater precision the angle $\gamma$ may be found by actually measuring the inclination to the vertical $\beta$ of the fringes in the ocular. Here if the height of image $s$ in the ocular corresponds to the vertical length of slit $S$,

$$\frac{s}{S}=\frac{f_t}{f_c}-2\left(1-\frac{D}{f_c}\right) \tag{23}$$

while

$$\beta=\frac{Nf_t}{s}\frac{d\theta'}{dn}$$

where $d\theta'/dn$ is given by equation 17. Hence $s$ may be eliminated and

$$\beta=\frac{N}{S\left(\frac{1}{f_c}-\frac{2}{f_t}+\frac{2D}{f_cf_t}\right)}\frac{d\theta'}{dn} \tag{24}$$

If now we further eliminate $N/S$ in equation 22 by equation 24, we have finally

$$\gamma=\frac{\beta\lambda(f_t+2(D-f_c))}{2f_cf_t(\cos\theta'-\cos i)d\theta'/dn}$$

so that $\gamma$ is given in terms of $\beta$, the observed inclination of fringes in the ocular. To measure $\beta$ the ocular must be revolvable on its axis, so that the cross-hairs may be brought into coincidence with the fringes and the angles may be found. To measure $M$, the $D$ lines as they remain vertical may often be used, if in focus, for reference in place of vertical cross-hairs.

Using the data of the above experiments, if $i=45°$—

| | | |
|---|---|---|
| $N=1$ | $f_c=f_t=D$ (nearly) $=23$ cm., | $\cos\theta'-\cos i=.2264$ |
| $S=.9$ cm. | $\lambda=60\times10^{-6}$ | $d\theta'/dn=493\times10^{-6}$ |

whence $\gamma=146\times10^{-6}$ radians, or about a half-minute of arc per fringe, and $\beta=44'$ per fringe. Thus $\beta$ is about 88 times as large as $\gamma$. At $i=22.5°$, $\gamma=1.5'$ per fringe, $\beta=45'$ per fringe. Naturally the sensitiveness increases with the angle of incidence $i$. When the fringes are large, one-tenth fringe is easily estimated, so that a horizontal angle $\gamma$ of a few seconds between mirror and grating should be measurable. An ocular micrometer, as suggested, would carry the precision beyond this.

**24. Summary.**—It has been shown that the interferences here in question take place in accordance with the equations (6), (7), and (8) above. They therefore occur in triplicate, but not necessarily in the same focus. Their superposition gives rise to fluted interference patterns of which the coarse fringes (8) are less sensitive to micrometer displacements than the fine fringes (6) and (7), on the one hand, while they persist over a comparatively greater range of path difference, on the other. The eventual sensitiveness of both approaches the wave-length of light. The adjustment made is essentially self-compensating, in a way that excludes the wedge-angle of the plate; and the lines are rigorously straight and vertical, to the extent in which they may be regarded as parts of the periphery of ellipses, whose centers are infinitely distant on the same horizontal. As a whole, therefore, these interferences are special cases of the phenomenon described in chapters IV and V, where they may be made to pass through the zero of air-space.

The lines are inclined for a wedge-shaped air-space in a manner admitting of the measurement of very small angles.

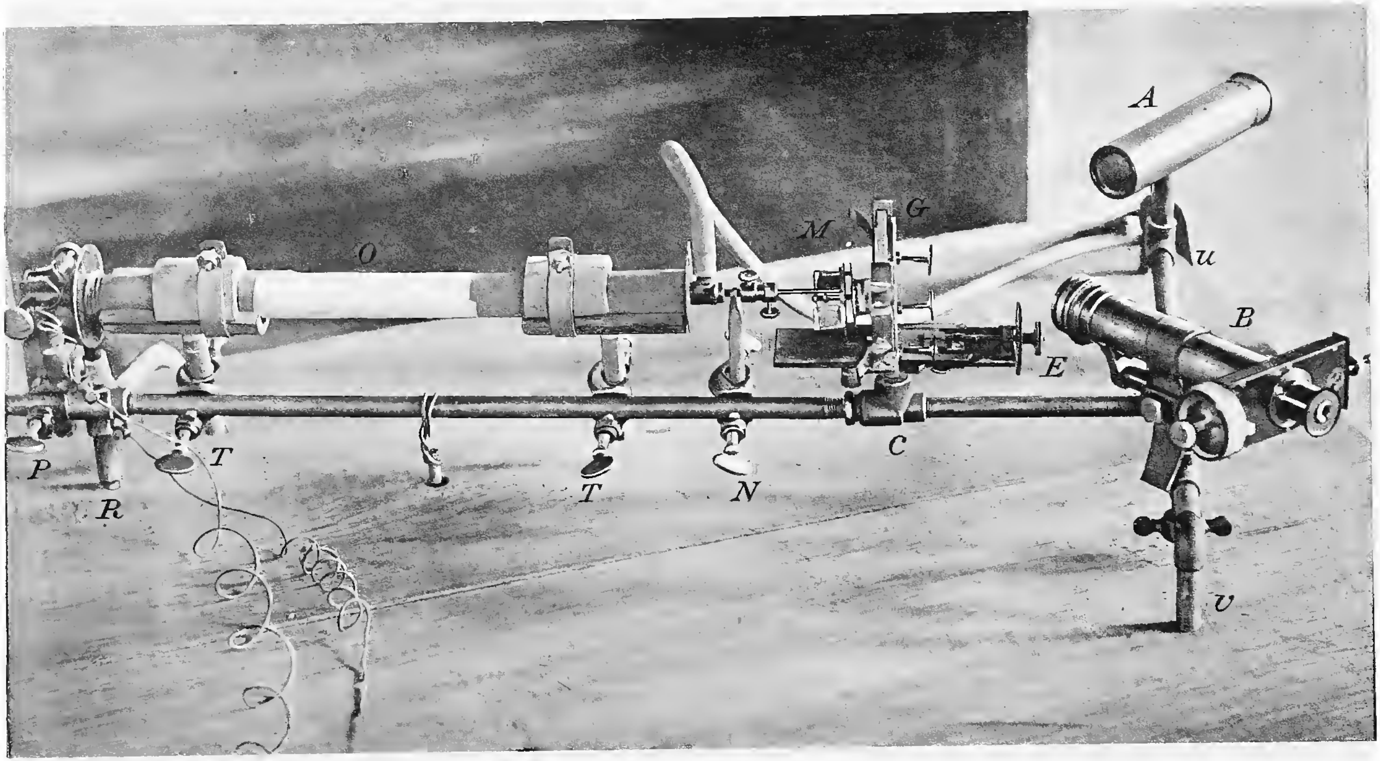


Fig. 10. Showing the Interferometer at $A$, $B$, $C$, and an attachment for Magnetostriction at $O$.

# CHAPTER III.

## THE GRATING INTERFEROMETER. By C. Barus and M. Barus.

**25. Introductory.**—In view of the perfection which has been attained in the construction of film gratings and of the simplicity of the instrumental equipment needed, we have been at some pains to put the type of interferometer recently described* into practical form. This is shown in the accompanying diagram, in which fig. 10 is a photographic view, the parts of which are easily recognized by aid of the simplified plan and elevation in fig. 11, A and B.

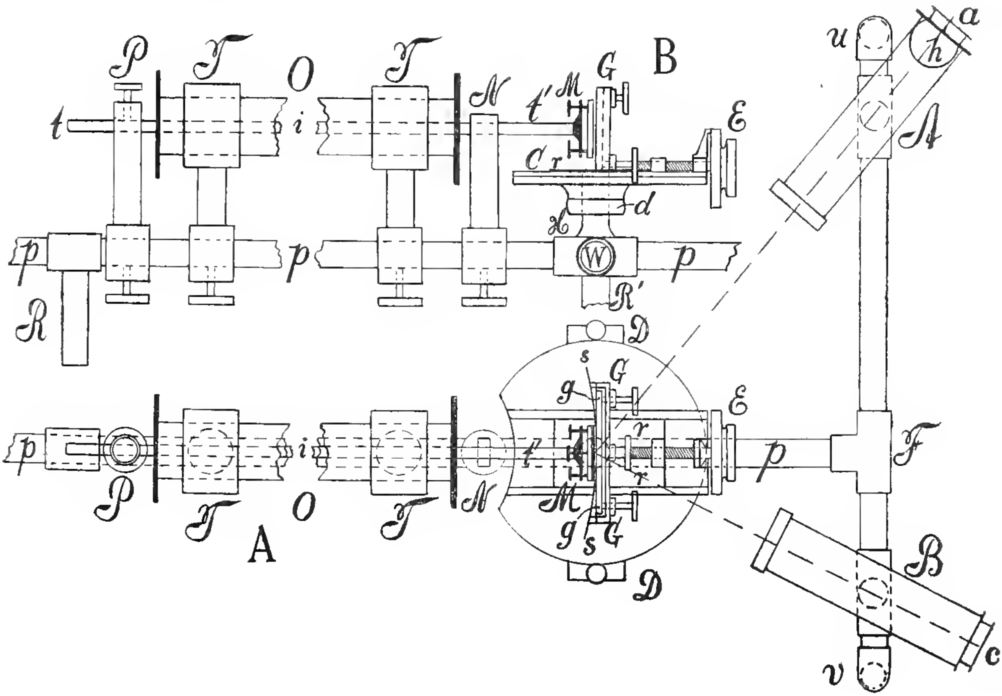

FIG. 11.—A. The same (fig. 10) in plan. B. The same in elevation.

The attachment for magneto-striction is purely incidental. The small increments of length in question were thought to offer an excellent test of the availability of the interferometer for micrometric length-measurements when these are of the sudden type and unlike the regular expansions.

* Science, xxxi, p. 394, 1910; Phil. Mag. (6), xx, p. 45, 1910; above chapter II.

**26. Apparatus.**—In fig. 11, *A* is the collimator, *B* the telescope for viewing the interference patterns reflected from the grating *gg* and mirror *M* over the revolvable table *CC*. These are the essential parts. The remainder is the incidental mounting just referred to, *O* being the helix containing an iron rod, soldered at its ends to brass or copper tubes, *t* and *t'*, the latter very light and movable in the V-groove *N*, the former *t* heavier and clamped in the upright *P*.

The whole is supported on a frame of quarter-inch gas piping and connections *uFvR*, the feet being at *uvR*, only the latter appearing in the figure. Under the grating is an attachment * with four or eight screw sockets, *W*, respectively at right angles to each other, into which a variety of apparatus may be screwed, in the absence of the removable pipe *pp*. When *p* is not used it is replaced by a foot.

Telescope *B* and collimator *A* are carried on T-pieces, with nipples at the same height (about 8 cm. or less) above the iron frame, and *B* may be slightly inclined about a horizontal axis. It may also be provided with a micrometer eyepiece, as shown in fig. 10.

The table, *CC*, carrying the grating, is revolvable on an upright *H* and may be clamped to fixed verniers, *D*, also carried at *d* by the upright *H*. The table is cut away on the further side so that vertical apparatus may approach closer to the grating in *GG*. It would even be an advantage to use (not much more than) a semicircular table with verniers *DD* alternately in use, set at an angle.

On the table two parallel brass guides determine the motion of the slide, *rr*, actuated by the micrometer screw *E*.

The grating is mounted with the film on a glass plate *gg*, and exposed on the side away from the observer, facing the mirror *M*. It is adjusted in a rectangular shallow brass case, *GG*, with the side toward *M* and the top open. The figure shows three adjustment screws actuating the rear of the glass plate, *gg*, and the springs *ss*, which push the plate to the rear, passing through slits in the sides of *GG*. There is one spring for the top and one for the bottom of the grating. The capsule *GG* is firmly attached to the slide *rr*, so that the grating may be moved fore and aft by the micrometer screw.

For some purposes the mirror *M*, similarly adjustable by three screws, may be attached to the plate *CC*, free from the slide *rr*. In the figure the mirror is on the light brass tube *t'*, which makes a prolongation of the iron rod, here to be tested for magneto-striction. The silvered face of *M* fronts the grating.

The coil, *O*, used is wound on a slender annular chamber or double tube, through which cold water may be kept in circulation (see fig. 10), to obviate changes of temperature of the rod. The uprights *P*, *T*, *T*, *N*, in figs. 10 and 11, moreover, are adjustable up and down as well as around the rod *pp*, by clamps shown in fig. 10, in which other unessential details may be seen, including the hose for supplying and removing water.

* In a later form a special base *R'* was provided below *W*.

**27. Adjustments.**—The micrometer screw controlled at $E$ has a double purpose. In the first place it is an immediate check on all measurements of length increment made. It shows, moreover, whether the displacements are expansions or contractions, since it may compensate any motion of the mirror. In the second place, since the collimator $A$ and telescope $B$ are clamped at a fixed distance apart approximately, it enables the observer to put the part of the spectrum needed into the center of the field. For the angle $aMc$ may here be considerably increased or decreased, and both telescopes are revolvable about the vertical. They may also be raised or lowered, moved right and left and rotated about the horizontal, being grasped by an ordinary clamp (not shown). The head $E$ of the screw, moreover, as well as the adjustment screws of the grating, are at all times within easy reach of the observer. After an initial rough adjustment (the direct reflections from mirror and grating being put into coincidence), the adjustment screws on the grating are manipulated until the three spectra seen in the telescope $B$ coincide both horizontally and vertically. For this purpose the $D$ and $E$ lines of the spectrum are useful and sunlight is preferable. In the absence of sunlight a small electric arc lamp with the rays issuing nearly parallel suffices equally well, supposing the apparatus is in adjustment. When telescope and collimator are fixed, motion at the micrometer screw naturally does not displace the spectrum line $\lambda$, on which the telescope has been focussed, so that the interferences recorded pass through a definite part of the spectrum.

The three sets of interferences available are subject to the equation

$$\delta e'' = \lambda/2 \cos i \qquad (1)$$

$$\delta e' = \lambda/2 \cos \theta \qquad (2)$$

$$\delta e = \lambda/2 (\cos \theta - \cos i) \qquad (3)$$

where $\lambda$ is the wave-length of light used, $i$ and $\theta$ the angles of incidence and of diffraction in air, and where $\delta e$, $\delta e'$, $\delta e''$, represent respectively the increment of air-space between mirror and grating per fringe passing the cross-hairs. It is therefore necessary to know the angles $\theta$ and $i$, and for this purpose the verniers $D$ and the revolvable plate $CC$ graduated on its edge are provided.

Let the mirror or grating plate be turned until the reflected image of the slit coincides with the slit itself. Here the observer must be able to look at the inner face of the slit in $A$ through the hole $h$ in the tube. Then let the angle be read off. Thereafter let the plate $C$ be unclamped and turned until the slit is seen sharply on the cross wire of the telescope $C$ and a second reading made. The angle so observed is $(i+\theta)/2 = a$. We may therefore write

$$\sin i - \sin \theta = 2 \cos (i+\theta)/2 \cdot \sin (i-\theta)/2 = \lambda/D$$

where $D$ is the grating space. Thus

$$\sin (i-\theta)/2 = \lambda/D \cos a$$

from which $(i-\theta)/2=b$ may be found. Hence $i=a+b$; $\theta=a-b$. An eccentric position of the grating is of no consequence.

In the given apparatus the inner angle of diffraction has been utilized. This brings $A$ and $B$ closer together for a sufficiently large angle $i$ to secure the best results.

In a later construction of the apparatus on an independent foot under $W$, $uv$ is a long smooth rod and $A$ and $B$ are attached by clamps admitting of motion right and left, up and down, and rotation about the horizontal and vertical.

**28. Angular extent of the fringes.**—In chapter II the equations were worked out (*l.c.*) for the more complicated case of a medium of thickness $e$ and refractive index $\mu$. For the case of an air-space the equations become much simplified. Corresponding to equations 1, 2, 3, if $\theta<i$ and $\sin i-\sin\theta=\lambda/D$

$$\frac{d\theta'}{dn}=\frac{\lambda^2}{2eD}\,\frac{1}{\cos i\cos\theta} \qquad (4)$$

$$\frac{d\theta''}{dn}=\frac{\lambda^2}{2eD}\,\frac{1}{1-\sin i\sin\theta} \qquad (5)$$

$$\frac{d\theta}{dn}=\frac{\lambda^2}{2eD}\,\frac{1}{1-\cos(i-\theta)} \qquad (6)$$

where $d\theta/dn$ is the angle subtended per fringe for the wave-length $\lambda$, the grating space $D$, the thickness of air-space $e$, at an angle of incidence $i$ and of diffraction $\theta$, in air.

These three sets need not be in focus at once. Equations 4 and 6 are usually easily put in focus together. Thus in the above case roughly,

$$i=50°\ 24' \qquad \theta=24°\ 44' \qquad \lambda/D=.352$$

whence for $\lambda=60\times10^{-6}$ cm. and $e=1$ cm.,

$$\frac{d\theta'}{dn}=.064' \qquad \frac{d\theta''}{dn}=.055' \qquad \frac{d\theta}{dn}=.378'$$

In case of the set of equations 4, 5, 6, therefore, there should be about 6 to 7 small fringes to one large fringe. This is about the order of values usually observed. When $e$ is small the change of wave-length with $d\theta$ must be considered. To obtain a given ratio $k$ of small and large fringe divergences, one may write for the cases 4 and 6, for instance,

$$k=2\,\frac{1-\cos(i-\theta)}{\cos(i-\theta)+\cos(i+\theta)} \qquad (7)$$

Equation 7 is not easily treated. If, however, $\theta$ is computed in terms of $i$ and expressed graphically, $k$ may then also be expressed in terms of $i$; and thus the angle of incidence $i$ for any ratio of size of fringes, $k$, in question, may be roughly adjusted. Table 7 shows these results.

TABLE 7.—Ratio of large and small fringes.

| $i$ | $\theta$ | $1/k$ | $1/k'$ | $i$ | $\theta$ | $1/k$ | $1/k'$ |
|---|---|---|---|---|---|---|---|
| 0° | −20° 1′ | 16.4 | 16.5 | 50° | 24° 27′ | 6.0 | 7.0 |
| 10 | −10 17 | 15.6 | 16.6 | 60 | 30 56 | 3.4 | 4.4 |
| 20 | − 0 34 | 14.8 | 15.8 | 70 | 36 0 | 1.6 | 2.6 |
| 30 | + 8 31 | 12.3 | 13.3 | 80 | 39 15 | .6 | 1.5 |
| 40 | 16 54 | 9.1 | 10.2 | 90 | 40 24 | .0 | 1.0 |

Thus it appears that at $i=37°$ about there should be ten small fringes to one large fringe. In a general way, moreover, the ratio of small to large fringes gives an estimate of the value of $i$.

Similarly equations 5 and 6 give

$$k'=2\frac{1-\cos(i-\theta)}{2-(\cos(i-\theta)-\cos(i+\theta))}$$

from which the data also given in table 1, follow.

Here there will be ten small to one large fringe when $i$ is 40.5° roughly.

The preceding equations 4, 5, and 6 are essentially approximate, inasmuch as the rates are taken for the finite quantities. If we return to the fundamental equations

$$2e\cos i=n\lambda \tag{8}$$

$$2e\cos\theta=n'\lambda \tag{9}$$

$$\sin\theta-\sin i=\lambda/D \tag{10}$$

for $\theta$ is greater than $i$, where $n$ and $n'$ are unequal distributive whole numbers; and if we put $e/D=a$, we find

$$\tan i=\frac{n^2-n'^2}{4an}-a \qquad \tan\theta=\frac{n^2-n'^2}{4an'}+a \tag{11}$$

which are free from $\lambda$, whereas $\sin i$ and $\sin\theta$ essentially contain $\lambda$. As the angular width of a fringe is

$$\theta=\int_n^{n+1}\frac{d\theta}{dn}\,dn$$

those corresponding to equations 4 and 5 may therefore be expressed as

$$\theta_1=2a\int_n^{n+1}\frac{-dn}{n\sqrt{n^2-4an\tan i-4a^2}} \tag{12}$$

$$\theta_2=2a\int_n^{n+1}\frac{-dn}{n(n-2a\tan i)} \tag{13}$$

for a given space $e$ in $a=b/D$ and a given angle of incidence $i$ in $\tan i$. These integrations are easily made, but the results are too diffuse to be worth discussing here. Equation 12, moreover, is a restatement of the fact that in these interferences $n\lambda$ is constant throughout the spectrum.

Equations 8, 9, and 10, however, admit of the graphic treatment of the problem. For if we put $A = nD/2e$, they may be written according as $\theta > i$ or $\theta < i$

$$\sin \theta_1 = \pm \frac{\cos i}{A} + \sin i \tag{14}$$

$$\sin \theta_2 = \frac{A^2 \sin i \pm \sqrt{1 + A^2 \cos^2 i}}{1 + A^2} \tag{15}$$

where the distributive number $n$ in $A$ takes the values of the successive whole numbers for a dark band in the respective spectra corresponding to equations 14 and 15. The coincidence of dark bands then determines the position of the coarse fringes.

If $i = 50^\circ\ 24'$

$$2e = .1 \text{ cm.} \qquad D = .000{,}169 \text{ cm.} \qquad \theta = 24^\circ\ 44'$$

then

$$A = .0017 \cdot n, \text{ nearly}$$

With these data table 8 was computed. Similar results might be computed for $\theta < i$, but I have abandoned it because, as is now evident, the practical demands are sufficiently met by the method of paragraph 28.

TABLE 8.—Showing $\theta_1$ and $n$, $\theta_2$ and $n'$. $\theta$ observed about 75°. $2e = 1$ cm., $i = 50.4°$, $\theta > i$. $\delta e$ corresponds to the mean value $\bar{\theta}$.

| $n$ | $\theta_1$ | $10^3\delta e_1$ | $\bar{\theta}_1$ | $n'$ | $\theta_2$ | $10^3\delta e_2$ | $\bar{\theta}_2$ |
|---|---|---|---|---|---|---|---|
| 1650 | 86.1° | 76 | 84.2° | 300 | 83.4° | 19 | 82.5° |
| 1700 | 82.3 | 46 | 81.2 | 400 | 81.5 | 18 | 80.5 |
| 1750 | 80.0 | 36 | 79.1 | 500 | 79.6 | 17 | 78.8 |
| 1800 | 78.2 | 30 | 77.6 | 600 | 77.9 | 16 | 77.1 |
| 1840 | 77.0 | 23 | 76.7 | 700 | 76.2 | 15 | 75.5 |
| 1870 | 76.3 | 30 | 75.8 | 800 | 74.7 | 14 | 74.0 |
| 1900 | 75.4 | 22 | 75.0 | 900 | 73.3 | 12 | 72.7 |
| 1940 | 74.5 | 20 | 74.2 | 1000 | 72.1 | .. | .... |
| 1970 | 73.9 | 20 | 73.6 | 2000 | 64.0 | .. | .... |
| 2000 | 73.3 | 18 | 73.2 | ... | .... | .. | .... |
| 2020 | 73.0 | 20 | 72.8 | ... | .... | .. | .... |
| 2040 | 72.6 | 15 | 72.5 | ... | .... | .. | .... |
| 2060 | 72.3 | . | .... | ... | .... | .. | .... |

**29. Test made by magneto-striction.**—The very small elongation produced when iron is magnetized offers an excellent test of the above apparatus. The attached water-cooled helix has already been described. The rod of Swedish soft iron was quite within the helix, which surrounded it closely without contact, the rod being prolonged by light copper tubes soldered to its ends.

A large number of experiments were made for trial, brief examples of which are given in the following table and charts, where if the current is in amperes the magnetic field

$$H = 108i \text{ gauss}$$

and the elongation $\delta e = 105 \times 10^{-6}$ cm. per large fringe. Thus if $n$ is the number of fringes and $l = 28$ cm. the effective length of the iron rod, the absolute elongation is $\delta a = 105n \times 10^{-6}$ cm. and the elongation per unit of length,

$$\delta\beta = 3.75n \times 10^{-6}$$

or if small fringes $N$ are taken,

$$\delta\beta = .54N \times 10^{-6}$$

Elongations from $10^{-6}$ cm. to $10^{-4}$ cm. were measured without difficulty, though such measurement, without micrometer attachment, is essentially an estimate. Count was made of the number of small fringes between the large fringes.

TABLE 9.—Magneto-striction elongations. Coil* (separated by thin sheet of flowing water from rod) length 37 cm., 3200 turns, $H = 108i$ gauss ($i$ in amperes). Swedish iron rod, diam., $2r = .64$ cm., length $l = 30.6$ cm., free length 28 cm. Elongations, $10^6 \delta e = 105$ cm., $10^6 \delta e_1 = 33$ cm., $10^6 \delta e_2 = 47$ cm. Seven small fringes to one large fringe.

| $H$ | Fringes. | $\delta\beta \times 10^8$ | $H$ | Fringes. | $\delta\beta \times 10^8$ |
|---|---|---|---|---|---|
| gauss | small | .... | gauss | small | .... |
| 13 | .0 | 0 | 98 | 6.0 | 320 |
| 22 | 1.5 | 79 | 56 | 7.0 | 370 |
| 36 | 4.0 | 210 | 36 | 5.0 | 310 |
| 44 | 6.0 | 320 | 23 | 2.0 | 110 |
| 62 | 7.0 | 370 | 9 | .0 | 0 |
| 62 | 6.5 | 350 | −9 | .5 | 26 |
| 44 | 5.5 | 300 | −23 | 3.0 | 160 |
| 36 | 5.0 | 270 | −36 | 5.5 | 300 |
| 13 | .0 | 0 | −56 | 6.0 | 320 |
| −13 | .5 | 26 | −99 | 5.0 | 270 |
| −22 | 3.5 | 190 | +99 | 5.0 | 270 |
| −62 | 7.0 | 370 | 69 | 6.0 | 320 |
| +62 | 7.0 | 370 | 56 | 6.0 | 320 |
| 13 | .5 | 26 | 19 | 1.2 | 64 |
| 6 | .0 | 0 | 11 | .0 | 0 |
| | | | −11 | .5 | 26 |

* A field of 150 gauss should more than practically saturate iron.

The data partake of the usual character of magnetic phenomena. There is marked hysteresis and irregularity due to residual magnetization. Table 9 has been inserted merely as an example of the results, which are otherwise given graphically. The maximum elongation corresponded to about 7 small fringes.

The curves bring out the following results consistently:

(1) The elongation apparently begins abruptly in small fields of 5 or 10 gauss, see fig. 12, etc., at $b$.

(2) In small fields, fig. 14, A, there is nevertheless a tendency of a very slow continual increase; but whether this is due to inevitable percussion during magnetization can not be stated. The case may be one of true magnetic elasticity.

(3) The maximum elongation is very rapidly reached in a field of 50 to 100 gauss. After this the elongation now due to strong fields decreases. In the case of strong fields, however, the rod as a whole is probably dis-

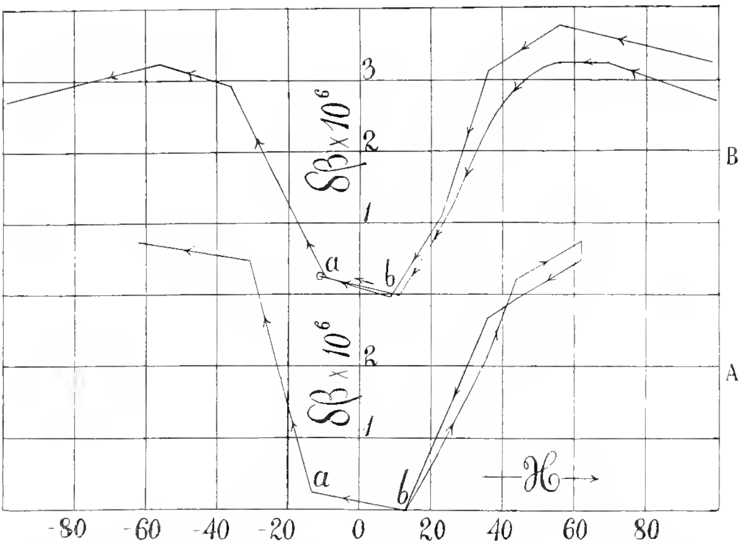


FIG. 12.—Charts showing the elongation of soft iron in millionths for different fields, positive and negative, in gauss. Field applied and removed for each observation.

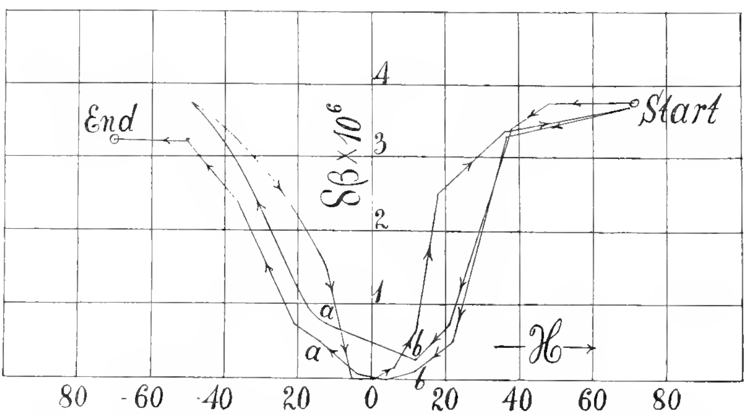


FIG. 13.—Chart showing the elongation of soft iron in millionths for different fields, positive and negative, in gauss. Field applied and removed for observation.

placed or warped. The results are less and less trustworthy and not suitable for exploration by the optic method in question (figs. 12, B, and 14, B and C).

(4) If the field is reversed the elongation is similar, but symmetrical with respect to a small positive field if the immediately preceding magnetization was positive, and symmetrical with respect to a small negative if the preceding magnetization was negative. See figs. 12, A, B, 13 (hysteresis). Thus in fig. 12, A and B, where a field of 13 gauss at $b$ after a positive magnetization produces no elongation whatever, the reversal of the field to $-13$ gauss produces a very marked elongation of nearly $3 \times 10^{-7}$ which

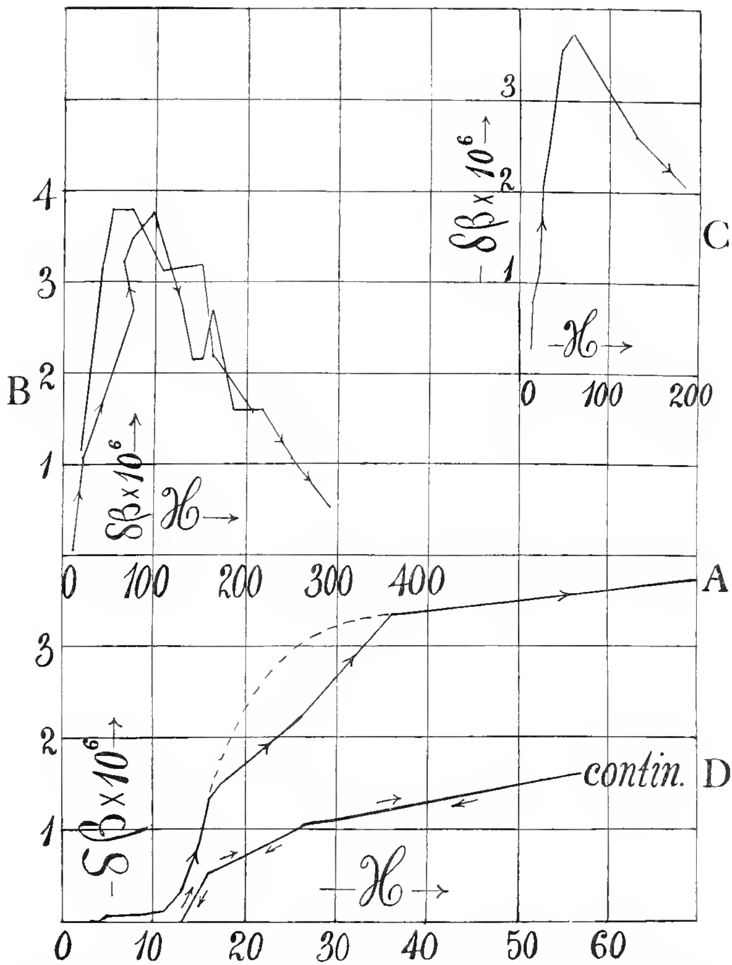


Fig. 14.—Charts showing the elongation of soft iron in millionths for different fields, positive and negative, in gauss. Field applied and removed for each observation except in fig. D.

may be repeated indefinitely. Hence there seems to be a definite magnetic elasticity with fields of less than 5 to 10 gauss. If this is exceeded the magnetic molecules are permanently set, even in soft iron.

(5) If the field varies continuously (liquid resistances) the elongations are much smaller in given fields (fig. 14, D).

The whole subject, which is here touched incidentally, is well summarized in Winkelmann's Handbuch, vol. 5, p. 307 *et seq.*, 1908, by Professor Auerbach. The above results agree closely with the elaborate experiments of Nagaoka and Honda,* who used a special type of contact lever. Recently Mr. Dorsey † has made a similar investigation, using an ingenious method of his own. The present method would not have been feasible but for the occurrence of large and small fringes in the field of the telescope.

**30. Summary.**—The present chapter has shown the ease with which the above phenomena may be adapted to the measurement of small displacements, has instanced their particular usefulness, inasmuch as fine and coarse adjustments are both available (recommending their use in the investigation of phenomena of sudden occurrence as in magneto-striction, etc.), and has given suggestions of practical forms of apparatus in addition to the usual spectrometric form.

* Nagaoka and Honda: Phil. Mag. (5), XXXVII, p. 131, 1894.
† Dorsey: Phys. Rev., XXX, p. 698, 1910.

## CHAPTER IV.

### THE USE OF THE GRATING IN INTERFEROMETRY; EXPERIMENTAL RESULTS.

**31. Introductory.**—In chapters II and III a method* was described of bringing reflected-diffracted and diffracted-reflected rays to interference, producing a series of phenomena which, in addition to their great beauty, promise to be useful. In fact, the interferometer so constructed needs but ordinary plate glass and replica gratings. It gives fringes rigorously straight, and their distance apart and inclination are thus measurable by ocular micrometry. Lengths and small angles are thus subject to micrometric measurement. Finally, the interferences are very easily produced and strong with white light, while the spectrum line used may be kept in the field.

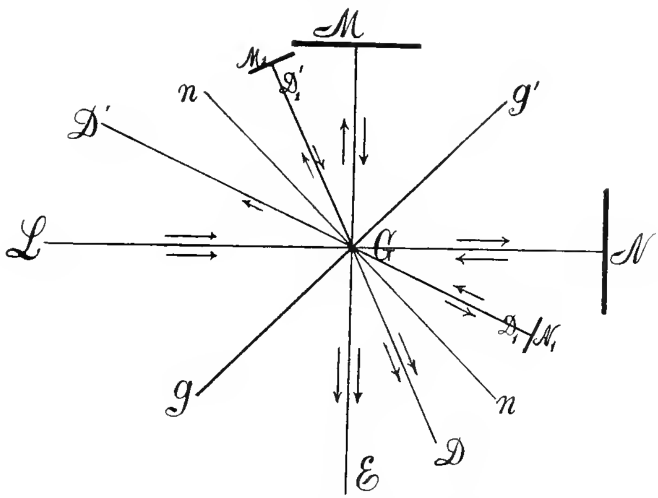


FIG. 15.—Diagram of grating interference adjustments adapted to Michelson's apparatus. *L*, source of white light (parallel rays), *gg'* grating, *M* and *N* opaque mirrors.

The same method is available as an adjunct to either Jamin's or Michelson's interferometers, except that here the transmitted-reflected-diffracted and reflected-transmitted-diffracted rays are brought to interfere. To take the example of the Michelson type, stripped of unnecessary details, let *gGg'* in fig. 15 be the grating or ruled surface, *n* its normal, *L* the source of white light, *M* and *N* the mirrors, and *E* the eye. In the usual way the rays from *L* interfere at *E*.

*Science, XXXII, p. 92, 1910; *cf.* Phil. Mag., July 1910, and chapters II and III above.

Now replace $L$ by a slit and collimator, $E$ by a telescope focussed for parallel rays. The eye at $E$ now sees a sharp line of light. At $D$ and $D'$, however, there must be two diffraction spectra coinciding in all their parts and hence interfering rhythmically, if all adjustments are sufficiently perfected. The other two diffractions within $MGg'$ and $EGg$ are often lost at an incidence of 45°

The attempt to produce these interferences at $D$, $D'$ with replica gratings is liable to result in failure; for while the transmitted system $NGD$ shows brilliant spectra, the reflected system $MGE$ is dull and hazy. Both spectra are clearly in evidence and may be brought to overlap. The film, however, does not reflect in a degree adequate to the transmission. Attempts made to realize the conditions of interference eventually, however, resulted in complete success (chapter V).

What is strikingly feasible at once, with ordinary plate glass and a non-silvered grating,* is the production of interferences between pairs of diffracted spectra, $D'$ and $D$, for instance, if returned by equidistant mirrors $M$ and $N$ to a telescope in the line $D$. Both of these spectra are very brilliant and not very unequally so and the coincidence of spectrum lines both horizontally and vertically brings out the phenomenon. This, for each of the cases specified, is of the ring type and not of the line type heretofore discussed; but it occupies the whole field of the spectrum from red to violet. One obtains brilliant large confocal ellipses with horizontal and vertical symmetry, and the spectrum lines, simultaneously in focus, may serve either as major or minor axes. The interferometer motion is twofold in character, consisting of radial motion, combined with a drift of the figure as a whole, in a horizontal direction. Naturally a fine slit is of advantage, but the experiment succeeds with quite a wide slit, especially in the red, much after spectrum lines vanish. Similarly the regular reflection from $M$ and $N$ (mirrors) will produce these phenomena along $GD$.

Such ellipses (I shall so call them, though they are probably ovals) as have their centers in the field, are clearly due to reflection from the same surface, as shown in fig. 15; curved lines or ellipses with remote centers are due to simultaneous reflections of the component rays from the opposite faces of the grating, since the angle of the wedge of glass can not be excluded. All owe their vertical and horizontal symmetry to the vertical slit and horizontal spectrum. The ellipses are identically present in the successive orders of spectra at once.

These elliptical fringes thus embody with the preceding linear set the common property of being duplex in character; only here the motion of dark rings to or from the centers of the ellipse, as a fine adjustment, is associated with a displacement of the fringes bodily through the spectrum (coarse adjustment).

* My thanks are due to Prof. J. S. Ames, of Johns Hopkins University, who was good enough to lend me this grating.

This displacement may be from red to violet or from violet to red, as the virtual air-space increases in thickness, depending upon the adjustment, as will presently appear. In other words, for a given small interferometer motion of mirror, there is in general less displacement of fringes bodily than radial motion of fringes to or from the center. Slight deflection of the grating, *gg'*, is chiefly accompanied by radial motion of the fringes.* The effect thus produced is to give sharpness to the interference pattern, which soon vanishes for approximate adjustments of spectra.

Similarly the micrometer screw produces a rapid passage of the pattern through its maximum size, a play of the screw of 0.1 cm. being sufficient to pass from fringes of one extreme of small size, through the maximum size to the final extreme. One may note that in chapters II and III the admissible play for the coarse fringes was about 1 cm., ten times greater. On the other hand there are many regions of interference; in fact, different groups of interferences may sometimes be in the field at once, or more usually corresponding to slightly different angles between the mirrors and grating.

All admissible angles, provided that symmetry is maintained (the virtual plane of the grating bisecting the angle of the mirrors), bring out the phenomenon. This points to the fact that the earlier phenomenon referred to (*l.c.*), in which the center or normal ray was virtually at an infinite distance, is now produced near an accessible center, even if this is not actually in the field. However, in the earlier case, when the angle of incidence is zero, curved lines may also be obtainable. Such cases will be given in the next chapter.

Experiments with a silvered grating showed no advantage, whether the transparent film covered the grating or the plane face of the glass. In fact, in case of good adjustment the phenomenon is so strong as to need no accessory treatment; this is in fact one of its advantages. A great difficulty in adjustment is the occurrence of stationary fringes due to the rear face of the grating. These may even wipe out the spectrum lines; but usually they lie at a finite focus and are not seen with a sharp spectrum. Fortunately many positions are available for obtaining the ellipses, so that a satisfactory one is easily found. Unless all overlapping spectra show sharp lines the adjustment is very tedious.† The amount of grating space used is less than 1 sq. cm., though of course a larger size is convenient for experiment.

**32. Special properties.**—The motion of the ellipses bodily across the spectrum, corresponding to the increased or decreased virtual air-space (micrometer screw), shows that whereas the vertical dimension or axes (direction of fixed color) do not appreciably change,‡ the horizontal axes

* This changes the effective thickness of the grating.

† These difficulties are largely removed by the method of coincident white slit images given in chapter V.

‡ Probably referable to increased refraction and decreased diffraction from red to violet.

grow rapidly smaller; *i.e.*, the ellipse is more eccentric from red to violet. With the grating used, however (about 2800 lines per centimeter), the major axis remained vertical, *i.e.*, the circular form was not reached throughout the first order even in extreme red.

It follows from this that in the second order the major axis of the ellipses for 2800 lines to the centimeter will probably be horizontal, and this was found to be strikingly true. The figure, moreover, is necessarily coarser and the lights and shadows in greater contrast. In the third order the ellipses are drawn out horizontally to a correspondingly greater degree. Thus it is clear that with a more dispersive grating the circular or even the horizontally elongated form must occur in the first order. Indeed with 6000 lines to the centimeter, ellipses occur in the red having horizontal major axis while the figure in the green is circular. Spectrum lines are very distinct, particularly in the second order. In all orders of spectra the centers of the ellipses are simultaneously on the same spectrum line and their vertical dimensions are about the same. Hence the spectrum lines may be used instead of cross-hairs, as they are fixed landmarks among the moving ellipses.

With replica gratings the center of the ellipses is usually remote, *i.e.*, reflection does not easily take place at the free grating surface. Apart from this the curved lines are good and strong. Samples must be tried out, in which the lines are as clear as possible in all the overlapping spectra. Six gratings of this kind were examined with about the same results. The centers of the ellipses could only rarely be brought into the field. Centers may, however, be obtained for gratings cemented under pressure between unequally thick plates of glass.

It has been stated that considerable width of slit is admissible. Moreover, the focal plane of the collimator (convergent or divergent light) or the focus of the telescope makes little difference, though the condition of parallel rays is naturally preferable. An eye focussed for infinity sees the fringes very well without the telescope and they may be also caught on a screen; but coming through a slit they are liable to be dark and the advantage of the telescope is obvious. The second order is particularly accessible for naked-eye observation, and the light and black appearance is accentuated, but they are liable to be irregular. Inclining the collimator moves the spectrum across the fringes vertically, while inclination of the telescope moves both equally. In this way the centers may often be found. With strong tipping, however, the figure becomes distorted or open above and below, as would be expected. If the light is intensified for projection or naked-eye work, there is also distortion.

It is not necessary (and apparently of little advantage) to have the reflections from the mirrors $M$ and $N$ occur at normal incidence. In fact the patch of white light on the grating surface and the return patch of spectrum may be over an inch apart. Inasmuch as the spectra are rigorously coincident, it follows that (apart from the refraction of the thick plate glass) the grating must be symmetrical with respect to the mirrors; *i.e.*, intersect the angle between them. Very little difference of size or shape is observable between extremes of such adjustment. Thus I rotated the grating about 10° (larger angles being unavailable) without appreciable effect, after one of the mirrors had been correspondingly adjusted.

On examination of the effective air-distances of the mirrors *M* and *N* from the grating, it is found that three positions are favorable to interference; in the first (case *A*), *M* is farther away than *N* from the corresponding faces of the glass plate; in the second (case *B*) they are about equidistant; finally, in the third (case *C*), *N* is further away, symmetrically with the first adjustment. For each case the admissible play of mirror (micrometer screw) does not much exceed 1 cm. for ordinary magnification. The second or equidistant adjustment brings out the lines or ellipses with distant centers, and there are usually three types easily found (after one has appeared), by slightly inclining either mirror around a horizontal axis by a tangent screw. Thus (see fig. 16) fine lines, say at 135° to the

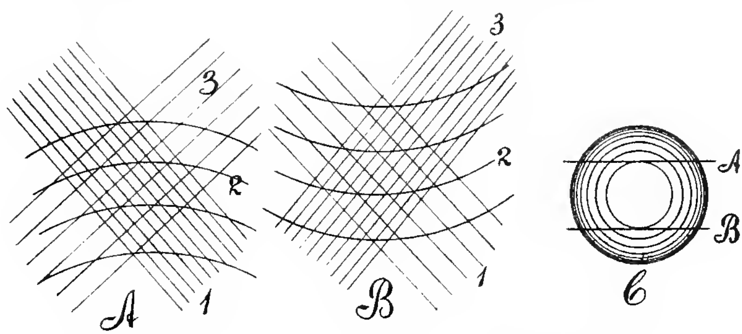


FIG. 16.—Interference patterns in case of self-compensation, *B*.

horizontal, coarse nearly circular lines, concave downward or upward as the case may be, and finally broad lines say 45° to the axis, may appear in succession. If the grating is rotated 180° around its normal, convexity upward (fig. 16, *A*) changesto concavity upward (fig. 16, *B*), showing the wedge angle of the glass plate to be effective. The micrometer-screw will pass any of these forms through a succession of inclinations corresponding to the eccentric intersection of a group of concentric circles by a straight line. This is also shown in fig. 16 at *A* and *B*, as observed for a fixed air-space and at *C*, on moving the micrometer in the *A* and *B* cases. These figures cover the coincident spectrum fields only. A solitary part of the field shows no interferences. For adjustment it is therefore necessary to cut off the spectra sharply above and below, by limiting the length of slit. Of the three or four spectra present the coincidence may then be secured with least difficulty. With each such coincidence there goes a definite position of the micrometer screw (interferometer), and this is the initial difficulty of adjustment; *i.e.*, to coordinate the various spectrum coincidences with the three screw readings.

The non-equidistant case of mirrors and grating correspond to the ring types with the centers in the field. Hence both reflections take place from the *same* face of the grating. When the distance *GM* is shorter, *G'N* longer, I have noticed two or even three ellipses successively in the field, obtained by slowly inclining the mirror *N* about the vertical (tangent screw), with their centers in turn in the yellow-green, the blue, and the green of the spectrum. They do not occur together. On turning the micrometer screw clockwise they move from red to violet, and vice versa.

When the distance *GM* is longer and *G'N* shorter, rings also occur; but only a single set was found. The spectrum lines not being clear, finding them was a matter of discrimination. When the micrometer screw was turned clockwise, however, they marched from violet to red, *i.e.*, in *opposite* direction to the preceding. The drift of ellipses corresponds with the direction in which the violet fringes move horizontally.

It is at first an astonishing result that when the grating is reversed (front face put rearward, leaving the air space unchanged) the ring type is left in the field; though the solitary ring type changes to the multiple type. This is true for the case specified as *A* or case *C*. It is also true for the eccentric type, case *B*, where line types, single or multiple, reappear at slightly different mirror angles. Briefly, rotation has no effect on the march of ellipses through the spectrum; but in case *B* it changes convex lines downward to concave lines, and vice versa. Nor has reversal of grating any effect on the march. The position of the grating with respect to the mirrors (three places being available) alone determines this result, certainly in the extreme cases *A* and *C*, and probably in the intermediate case *B*.

The use of a compensator in either of the component rays is always accompanied by the two effects in question; *i.e.*, there is both relatively large radial motion of the fringes and relatively small displacement, within the field of the telescope. One may therefore be evaluated in terms of the other, the two having the stated relation of coarse and fine adjustments. In case *B* the fringes will rotate, expand, or contract.

**33. Elementary theory.**—The endeavor must now be made to explain these results more in detail. For this purpose fig. 17 may be consulted.

In the grating used at an incidence of about 45° the angle of diffraction in the first order was about 32° 39′ for the $D_2$ sodium line, there being about 2847 lines to the centimeter, corresponding to a grating space of $D = .0003512$ cm. Thus $\lambda/D = 0.1677$. The index of refraction was assumed to be 1.53 for the same line.

The diagrams are drawn for an angle of incidence of 45° and for normal reflection from the mirrors *M* and *N*. In case of the grating given, the three positions of the grating at which interferences occur were about 0.6 cm. apart and are marked 124, 100, and 76 scale parts, on the micrometer screw normal to the grating. In other words it was convenient to move the grating at the center of the spectrometer, rather than the mirrors $M$ and $N$ adjustably attached near the edge of the plate graduated in degrees.

In group $A$ at 124 the short air-path is to $M$, the long path to $N$; in group $C$ at 76 the reverse is true. In group $B$ at 100, the system is self-compensating and the air-paths about equal.

In all cases the angle of diffraction, $\theta$, is less than the angle of incidence, $i$. There are of course corresponding cases, $\theta > i$, which have not been drawn, because they merely duplicate the cases given, at a different angle. It is assumed that after more than one direct reflection or one diffraction the interferences are no longer observable.

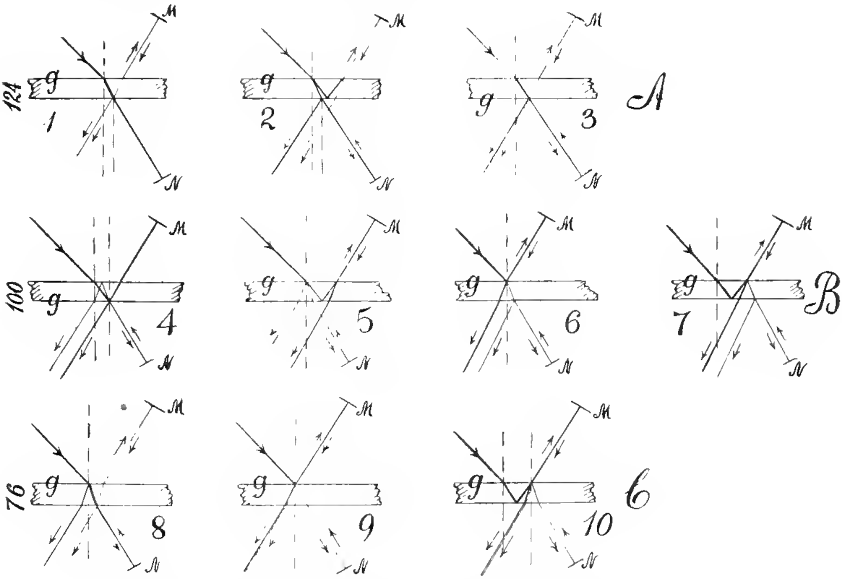


FIG. 17.—Chart of the three groups of interferences, $A$, $B$, $C$. Mirrors $M$ and $N$ return the spectrum. Grating face in position shown at $g$.

The diagrams 124 and 76 show that the two reflections of the component rays at the grating take place at the same surface; hence the occurrence of centered figures or rings. On the contrary the reflections in diagram 100 take place at the two different faces of the grating respectively; hence the angle of the grating is included and liable to produce eccentric ring systems. The center may be so far off that the dark lines are nearly straight, but they change their inclination as the vertical projection of the center moves horizontally through the field.

Some of these cases may coalesce in practice or they may destroy each other more or less. I have taken a single incident ray from which may come two parallel emergent rays, which are brought to interfere by the telescope. It would have been just as convenient to have taken the two corresponding incident rays which interfere in a single emergent ray. From the position of the mirrors it is clear that the regularly refracted rays are not returned. Only rays *first diffracted* at the grating (where they may also be reflected) are returned by the mirrors.

As a whole we may distinguish two typical cases, those in which both component rays are diffracted as in No. 1 or refracted as in No. 2; and those in which one component ray is refracted and the other diffracted. If $i$ and $\theta'$ are the angles of incidence and diffraction in air and $r$ and $\theta$ the corresponding angles of refraction and diffraction in glass, the glass path differences, $\Delta x$, in the important cases are as follows:

| | | | |
|---|---|---|---|
| No. 1. | $\Delta x = 2\mu e/\cos\theta = 2.2$ cm. | No. 7. | $\Delta x =$ Zero. |
| 3. | $= 2\mu e/\cos\theta = 2.2$ cm. | 8. | $=$ Zero. |
| 4. | $=$ Zero. | 9. | $= -2\mu e/\cos\theta = 2.2$ cm. |
| 6. | $=$ Zero. | 10. | $= -2\mu e/\cos\theta = 2.2$ cm. |

Here $\mu$ is the index of refraction and $e$ the thickness of the glass plate of the grating, and excess of path for the $M$ ray is reckoned positive. These paths must be compensated by corresponding decrements and increments respectively of the air paths $GM$ and $GN$. Ordinarily these path differences in glass being fixed for given angles $\theta'$ would fall away; but they vary essentially with color and hence the degree of compensation is never the same for all colors.

Furthermore, although the wave-fronts of the two rays are the same on emergence, this does not imply coincidence of phase even in such cases as Nos. 1 and 2, for instance; the absolute lengths of paths in glass are quite different, although their differences are the same. Consequently the cases 1 and 2 would again interfere if superimposed, one case being first diffracted and the other first refracted.

Thus it is not surprising that so many cases were identified. It is also apparent that the air compensations are very different and hence identification is facilitated. Finally, since a vertical slit and collimator are used, the section of a beam of light passing through the grating by a horizontal plane consists of parallel rays; the section by a vertical plane, however, is convergent.

It is interesting to find the numerical data for the above equations, assuming that

$$i = 45^\circ \qquad \theta' = 32^\circ\, 39' \qquad e = .68 \text{ cm.} \qquad \mu = 1.53 \text{ (estimated)} \qquad \lambda/D = .1677$$

for the sodium line of the spectrum. The results are given with the equations. Their value is about 2.2 cm., which is equivalent to a displacement of mirror actually found.

It follows, moreover, that the center of the ring system, order $n = 0$, must move from red to violet or the reverse, inasmuch as the compensation takes place successively, at each color, in the same way. Although the equations hold only for the center, and the symmetrically oblique rays belonging to the rings have not been given consideration, an approximate computation of the motion of the ring centers may nevertheless be attempted.

From the equations qualitative interpretations of the above and the following data are obtainable; but quantitatively they are too crude, because they ignore the essential feature of oblique reflection from $M$ and $N$.

Omitting these equations, to be fully discussed in the next chapter, an example of the displacement and radial motion in a given experiment may be adduced; the former was fully 16 times less sensitive per fringe than the latter. The displacement is thus a coarse adjustment in comparison with the usual radial motion of the fringes and this is the distinct advantage of the present method for many purposes. It is like a scale division into smaller and larger parts, where the enumeration of small parts alone would be confusing or impossible. The ratio of the micrometer value of displacement and radial motion per fringe may be given any value since $dz/d\lambda \propto e$ and the lateral displacement may actually be more sensitive than the radial motion, when the grating plate is thin.

The sodium lines here make admirable cross-hairs and the ocular itself need have none. The conditions are the same in the second order and the coarser rings and spectrum lines are often easier to count.

**34. Compensator.**—It is not necessary, however, to use thin glass, for if a compensator is provided, *i.e.*, if the grating is on the common plane between two thicknesses of identical plane-parallel glass plates, one of which carries the grating, the ideal plane in question is provided. The ellipses in this case would be infinite in size and their displacements infinitely large. By partial compensation (compensator thinner) ellipses of any convenient size and rate of displacement may therefore be provided at pleasure. The following table gives some rough experimental data where $z$ is the advance of the micrometer screw normal to the grating, *i.e.*, the displacement of the grating to move the center of fringes from the $D$ to

TABLE 10.—Displacement of ellipses from the $D$ to the $b$ line, by moving the grating $\Delta z$ cm. normal to itself. $i=45°$, nearly. Grating: $e=.68$ cm., $D=.000351$ cm., $\mu=1.53$ (estimated). Compensation shown by negative sign. Position $z$ taken while the sodium line was the major axis.

| Compensator thickness* $e' \times 10^2$ | Position of grating $z$ | Micrometer displacement $\Delta z \times 10^4$ | No. of fringes $D$ to $b$ | Displacement per fringe $10^4 \times dz/dn$ | Ellipses. | Side of compensator. |
|---|---|---|---|---|---|---|
| *cm.* | *cm.* | *cm.* | | *cm.* | | |
| −48 | .05 | 30 | 12 | 2.5 | Very large.... | N |
| −44 | .08 | 35 | ... | ... | Very large.... | N |
| −29 | .12 | 45 | ... | ... | Large........ | N |
| −10 | .20 | 65 | ... | ... | Mean........ | N |
| +48 | .38 | 115 | 44 | 2.6 | Very small... | M |
| −65 | .00 | 10 | 4.5 | 2.3 | Enormous.... | N |
| ± 0 | ... | 70 | 28 | 2.5 | Mean........ | None |

*Compensator parallel to mirror, $M$ or $N$, respectively.

the *b* lines of the spectrum, $e'$ the thickness of the compensator placed parallel to the mirror $M$ or $N$ as stated.

Rotation of the compensator offers the usual easy method of adjustment. In the second order the first rings, on compensation, usually more than fill the field. This is of course eventually the case in the first order also. With very perfect compensation the ellipses are quite eccentric and the lines under the limiting conditions nearly vertical and straight. Hence their motion, partaking of the twofold character specified, is complicated but usually opposite in direction on the two sides of the center for the same micrometer displacement. The whole phenomenon may vanish within a half millimeter of play of the grating, passing from fine lines through enormous ellipses back into reversed fine lines, all nearly vertical.

The displacement of the grating by the micrometer screw is of the same order per fringe, no matter whether the ellipses are large or small, and in the last table it was about .00025 cm. per fringe. The displacement at the mirror would exceed this. The radial motion per fringe is of the order of wave-length. Naturally the position $z$ of the grating changes parallel to itself linearly with the thickness $e'$ of the compensator, supposing other conditions the same, so that $p$, $z$, and $dz/dn$ all vary linearly with $e'$ the thickness of the compensator.

The full equations for the amounts of displacement, etc., require an evaluation of $d\theta/dn$, which in turn must take into consideration that reflection from the mirrors can not in general be normal except for the one color instanced above. This investigation will have to be reserved for the next chapter.

# CHAPTER V.

## INTERFEROMETRY WITH THE AID OF A GRATING; THEORETICAL RESULTS. By Carl Barus.

### Part I. Introduction.

**35. Remarks on the phenomena.**—In the earlier papers* I described certain of the interferences obtained when the oblique plate *gg*, fig. 18, of Michelson's adjustment, is replaced by a plane diffraction grating on ordinary plate glass. Some explanation of these is necessary here. In the figure *L* is the source of white light from a collimator. Such light is therefore parallel relative to a horizontal plane, but convergent relatively to a vertical plane. *M* and *N* are the usual silver mirrors. A telescope adjusted for parallel rays in the line *GE* must therefore show sharp white images of the slit. As the grating is usually slightly wedge-shaped, there will be (normally) four such images, two returned by *M* after reflection from the front (white) and rear face (yellowish) of the plate *gg*, and two due to *N*. There will also be two other, not quite achromatic, slit images from *N* or *M*, respectively, due to *double* diffraction before and after reflection. These will be treated below. In the direction *GD* there will thus be a corresponding number of diffraction spectra, more or less coincident in all their parts, and therefore adapted to interfere in pairs throughout their extent. If the two white and the two yellow images of the slit be put in coincidence and the mirrors *M* and *N* are adjusted for the respective *reduced* or virtual path difference zero, the interferences obtained are usually eccentric; *i.e.*, the centers of the interference ellipses are not in the field of view. The effective reflection in each of these cases takes place from the front and rear face of the grating at the same time. Hence the interference pattern includes the prism angle of the grating plate and is not centered. The air-paths of the component rays are here practically equal. In addition to the ellipses, this position also shows revolving linear interferences and (as a rule) a double set is in the field at once, consisting of equidistant, symmetrically oblique crossed lines, passing through horizontality in opposite directions together, when either mirror *M* or *N* is slightly displaced.

If either pair of the white and yellowish images of the slit be placed in coincidence when looking along *EG*, the interference pattern along *DG* is ring-shaped, usually quasi-elliptic and centered. The light returned by *M* and *N* is in this case reflected from the *same* face of the grating, either from the face carrying the grating or the other (unruled) face. The corresponding air-paths of the rays are in this case quite unequal, because the

* Am. Journ. of Science, xxx, 1910, pp. 161–171; Science, July 15, 1910, p. 92; and Phil. Mag., July, 1910, pp. 45–59.

short air-path is compensated by the path of the rays within the glass plate. Hence these adjustments are very different, *GM* being the long path in one instance, *GN* in the other instance. For the same motion of the micrometer screw, the fringes are displaced in opposite directions. In one adjustment there may be a single family of ellipses; in the other there may be two or even three families nearly in the field at once.

If the grating were cut on optical plate glass, the adjustment for equal air-path would probably be best. But with the grating cut as usual on ordinary plate, or in case of replica gratings on collodion or celluloid films, the adjustment for unequal paths is preferable. Here again one of the positions is much to be preferred to the other, owing to the occurrence of multiple slit images from one of the mirrors, as above specified. In fig. 19, for instance, where the grating face is to the rear, there are but two images, 1 and 2 from *M*, if the plate is slightly wedge-shaped; but from *N*, in

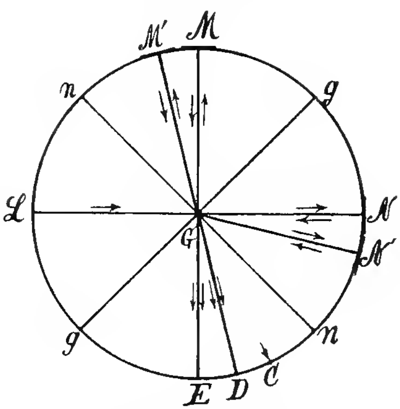


FIG. 18.—Diagram showing adjustments for interference.

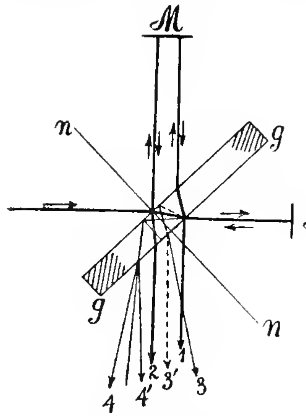


FIG. 19.—Diagram showing double diffraction.

addition to these two normal cases (not necessarily coinciding with 1 and 2), there are two other images $3'$ and $4'$ (3 and 4 are spectrum rays), resulting from double diffraction, with a deviation $\theta$ and angle of incidence $I$, respectively $\theta < I$ and $\theta > I$, in succession; or the reverse. As the compensation for color can not here be perfect, the two slit images obtained are very narrow, practically linear spectra, but they are strong enough to produce interferences like the normal images of the slits, with which they nearly agree in position. Other very faint slit images also occur, but they may be disregarded. The doubly-diffracted slit images are often useful in the adjustments for interference.

Among the normal slit images there are two, respectively white and yellowish, which are remote from secondary images. If these be placed in coincidence both horizontally and vertically along *EG*, fig. 18, the observation along *DG* through the telescope will show a magnificent display of black apparently confocal ellipses, with their axes respectively horizontal and vertical, extending through the whole width of the spectrum, from red to violet, with the Fraunhofer lines simultaneously in focus. The vertical axes are not primarily dependent on diffraction and are therefore of about the same angular length throughout; the horizontal axes, however, increase with the magnitude of the diffraction, and hence these axes increase from violet to red, from the first to the second and higher orders of spectra, and in general as the grating space is smaller. It is not unusual to obtain circles in some parts of the spectrum, since ellipses which in one extreme case have long axes vertically, in the other extreme case have long axes horizontally. The interference figure occurs simultaneously in all orders of spectra, and it is interesting to note that, even in the chromatic slit images shown in fig. 19, needle-shaped vertical ellipses are quite apparent.

It is surprising that all these interferences may be obtained with replica or film gratings, though not of course so sharply as with ruled gratings, the ideal being an optical plate. With thin films two sets of interferences are liable to be in the field at once and I have yet to study these features from the practical point of view. If the film is mounted between two identical plates of glass, rigorously linear, vertical and movable interference fringes, as described* by my son and myself, may be obtained.

**36. Cause of ellipses.**—The slit at $L$, fig. 18, furnishes a divergent pencil of light due (at least) to its diffraction, the rays becoming parallel in a horizontal section after passing the strong lens of the collimator. But the vertical section of the issuing pencil is essentially convergent. Hence if such a pencil passes the grating the oblique rays relatively to the vertical plane pass through a greater thickness of glass than the horizontal rays. The interference pattern, if it occurs, is thus subject to a cause for contraction in the former case that is absent in the latter. Hence also the vertical axes of the ellipses are about the same in all orders of spectra. They tend to conform in their vertical symmetry to the regular type of circular ring-shaped figure as studied by Michelson and his associates and more recently by Feussner,† but in view of the slit the symmetry is cylindric.

On the other hand the obliquity in the horizontal direction, which is essential to successive interferences of rays, is furnished by the diffraction of the grating itself, as the deviation here increases from violet to red. In other words the interference which is latent or condensed in the normal white linear image of the slit is drawn out horizontally and displayed in the successive orders of spectra to right and left of it. The vertical and horizontal symmetry of ellipses thus follows totally different laws, the former of which have been thoroughly studied The present paper will therefore be devoted to phenomena in the horizontal direction only.

* Phil. Mag., *l.c.*

† See Professor Feussner's excellent summary in Winkelmann's Handbuch der Physik, vol. 6, 1906, p. 958 *et seq.*

At the center of ellipses the *reduced* path difference is zero; but it can not increase quite at the same rate toward red and violet. Neither does the refractive index of the glass admit of this symmetry. Hence the so-called ellipses are necessarily complicated ovals, but their resemblance to confocal ellipses is nevertheless so close that the term is admissible. This will appear in the data.

If either the mirror or the grating is displaced parallel to itself by the micrometer screw the interference figure *drifts* as a whole to the right or to the left, while the rings partake of the customary motion toward or from a center. The horizontal motion in such a case is of the nature of a coarse adjustment as compared with the radial motion, a state of things which is often advantageous—in other words, the large divisions of the scale are not lost; moreover the displacements may be used independently.

The two motions are coordinated, inasmuch as violet travels toward the center faster in a horizontal direction, *i.e.*, at a greater angular rate, than red. Hence the ellipses drift horizontally but not vertically. Naturally in the two positions specified above for ellipses, the fringes travel in opposite directions for the same motion of the micrometer screw. As the thickness of the grating is less the ellipses will tend to open into vertical curved lines, while their displacement is correspondingly increased. With the grating on a plate of glass about $e=.68$ cm. thick and having a grating space of about $D=.000351$ cm., at an angle of incidence of about 45°, the displacement of the center of ellipses from the $D$ to the $E$ line of the spectrum corresponded to a displacement of the grating parallel to itself of about .006 cm. It makes no difference whether the grating side or the plane side of the plate is toward the light or which side of the grating is made the top. If the grating in question is stationary and the mirror $N$ alone moves parallel to itself along the micrometer screw, a displacement of $N=.01$ cm. roughly moves the center of ellipses from $D$ to $E$, as before. This displacement varies primarily with the thickness of the grating and its refraction. It does not depend on the grating constant. Thus the following data were obtained with film gratings on different thicknesses $e$ of glass and different grating spaces $D$ for the displacements $N$ of the mirror at $N$, to move the ellipses from the $D$ to the $E$ line, as specified.

| | | | |
|---|---|---|---|
| Glass grating, ruled. . . . . | $e=.68$ cm. | $\lambda/D=.168$ | $N=.010$ cm. |
| Film on glass plate . . . . . | $e=.57$ | .352 | .008 |
| Film on glass plate . . . . | $e=.24$ | .352 | .003 |
| Film between glass plates. | $\left\{\begin{matrix} e=.48 \\ e'=.24 \end{matrix}\right\}$ | .352 | .003 |

Reduced linearly to $e=.68$ cm., the latter data would be $N'=.010$ and $N'=.009$, which are of the same order and as close as the diffuse interference patterns of film gratings permit. The large difference in dispersion, together with some differences in the glass, has produced no discernible effect.

An interesting case is the film grating between two *equally* thick plates of glass. With this, in addition to the elliptical interferences above described, a pattern of vertical interferences identical with those discussed in a preceding paper* was obtained. These are linear, persistently vertical fringes extending throughout the spectrum and within the field of view, nearly equidistant and of all colors. Their distances apart, however, may now be passed *through* infinity when the virtual air-space passes through zero; and for micrometer displacements of mirror in a given direction, the motion of fringes is in opposite directions on different sides of the null position of the mirror. I have not been able, however, to make them as strong and sharp as they were obtained in the paper specified.

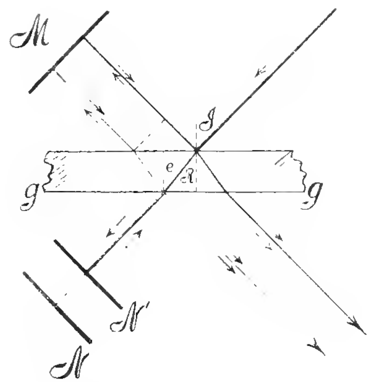


FIG. 20.—Diagram showing displacement of mirror $N$.

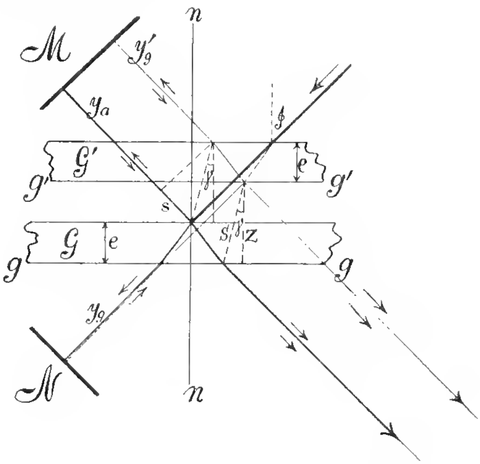


FIG. 21.—Diagram showing displacement of grating $G$.

**37. The three principal adjustments for interference.**—To compute the extreme adjustments of the grating when the mirror $N$ is moved, fig. 20 may be consulted. Let $y_g$ be the air-path on the glass side, whereas $y_a$ is the air-path on the other, $e$ the thickness of the grating and $\mu$ its index of refraction for a given color. Then for the simplest case of interferences, in the first position $N$ of the mirror, if $I$ is the normal angle of incidence and $R$ the normal angle of refraction for a given color,

$$y_g + e\mu/\cos R = y_a$$

for equal paths. Similarly in the second position of the mirror

$$y_a' = y_g' + e\mu/\cos R$$

Hence if the displacement at the mirror $N$ be $N$,

$$N = y_a - y_g = 2e\mu/\cos R + y_g' - y_a$$

The figure shows

$$y_a - y_g' = 2e \tan R \sin I$$

whence

$$N = 2e\mu \cos R$$

* Phil. Mag., *l.c.*

The measurement of this quantity showed about 1.88 cm. The computed value would be $2\times.68\times1.53\times.71=1.84$ cm. The difference is due to the wedge-shaped glass which requires a readjustment of the grating for the two positions.

The corresponding extreme adjustments, when the grating *gg* instead of a mirror *N* is moved over a distance *z*, are given in fig. 21. The mirrors *M* and *N* are stationary. It is first necessary to compute $\gamma$, the angle between the displacement *z* and the side *S* in the figure, or

$$\tan\gamma=\tan I-2e\tan R/z$$

so that the semi-air-path difference of rays to the mirror *M* becomes

$$s=y_a-y_g'=z(\cos I-\sin I\tan\gamma)$$

We may now write, with the same notation as before, for the extreme position of the grating, *G* and *G'*, respectively,

$$y_g+e\mu/\cos R=y_a \qquad y_a'=y_g'+e\mu/\cos R$$

or

$$z/\cos I=2e\mu/\cos R-z(\cos I-\sin I\tan\gamma)$$

whence

$$z(1/\cos I+\cos I-\sin I\tan\gamma)=2e\mu/\cos R$$

If $e=0$, it follows that $z=0$, or $\gamma=I$, since the parenthesis by the above equation is not zero. There is only one position. The angle $\gamma$ may now be eliminated by inserting $\tan\gamma$, whence

$$z=\frac{e\mu}{\cos I\cos R}-e\tan I\tan R$$

The observed value of *z* for the two positions was about 1.3 cm. The computed value for $I=45°$ is the same.

On the other hand, when reflection takes place from the same face of the grating, while the latter is displaced *z* cm. parallel to itself, the relations of *y* and *z* for normal incidence at an angle *I* are obviously

$$y\cos I=z$$

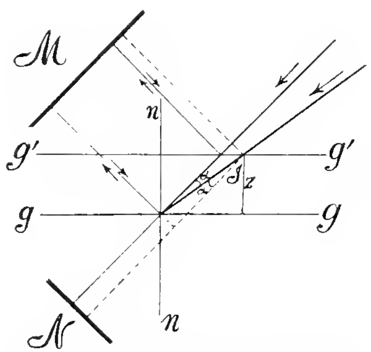


FIG. 22.—Diagram showing displacement of grating for deviated rays.

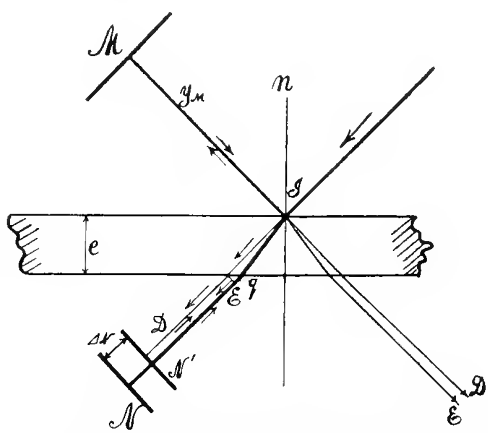


FIG. 23.—Diagram showing displacement of mirror *N* for different colors.

For an oblique incidence $i$, where $i-I=\alpha$, a small angle, the equation is more complicated. Fig. 22, for $e=0$, $g$ and $g'$ being the planes of the grating, shows that in this case

$$y=z(1+2\frac{\sin\alpha}{\cos i}.\sin I)/\cos I$$

or, approximately for small $\alpha$

$$y=z(1+2\sin\alpha\tan I)/\cos I$$

This equation is also true for a grating of thickness $e$, whose faces are plane parallel, for the direction of the air-rays in this case remains unchanged.

Finally, a distinction is necessary between the path difference $2y$ and the motion of the opaque mirror $2N$, which is equivalent to it, since the light is not monochromatic. This motion $2N$ is oblique to the grating and if the rays *differ in color* further consideration is needed. In fig. 23 for the simplest type of interferences, in which the glass-path difference is $e\mu/\cos R$ and for normal incidence at an angle $I$, let the upper ray $y_M$ and the grating be fixed. The mirror moving over the distance $\Delta N$ changes the zero of path difference from any color of index of refraction $\mu_D$ to another of index $\mu_E$, while $y_{ND}$ passes to $y_{NE}$. Then

$$y_M=y_{ND}+e\mu_D/\cos R_D=y_{ND}+e\mu_E/\cos R_E+\Delta N$$

Hence

$$\Delta N=-e\sin I\ (\tan R_D-\tan R_E)+e\left(\frac{\mu_D}{\cos R_D}-\frac{\mu_E}{\cos R_E}\right)$$

or

$$\Delta N=e(\mu_D\cos R_D-\mu_E\cos R_E)$$

This difference belongs to all rays of the same color difference, or for two interpenetrating pencils.

If reflection takes place from the lower face the rays are somewhat different, but the result is the same. If the plate of the grating is a wedge of small angle $\varphi$, the normal rays will leave it on one side at an angle $I+\delta$ where $\delta$ is the deviation

$$\delta=(\mu-1)\varphi$$

The mirror $N$ will also be inclined at an angle $I+\delta$, to return these rays normally. We may disregard $d\delta=\varphi d\mu$, if $\varphi$ is small.

## Part II. Direct Cases of Interference. Diffraction Antecedent.

**38. Diffraction before reflection.**—If in fig. 18 the diffracted beams (spectra) be returned by the mirrors $M'$ and $N'$ to be reflected at the grating, interference must also be producible along $GD$. Again there will be three primary cases: if reflection takes place from both faces of the grating at once, the air-paths must be nearly equal, the grating itself acting as a compensator. The interference pattern is ring-shaped, but as usual very eccentric. If the reflection of both component beams takes place from the same face of the grating, the interference pattern is elliptical and centered and the air-paths are unequal. The case is then similar to the preceding §§1, 2; but there is no direct or normal image of the slit, as $M$ and $N$ are absent. In its place there may be *chromatic* images of the slit (linear spectra) at $C$ due to the *double* diffraction of each component beam in a positive and negative direction successively. But these chromatic images are nevertheless sharp enough to complete the adjustments for interference by placing the slit images in coincidence. It is not usually necessary to put the spectrum lines into coincidence separately (both horizontally and vertically), as was originally done, both spectra being observed. Again along $GE$, fig. 18, approximately, there must be two successive positive diffractions of each component beam, which would correspond closely to the second order of diffraction. The advantage of this adjustment lies in the fact that there are but two slit images effectively returned by $M'$ and $N'$, and hence these interferences were at first believed to be stronger and more isolated. As a consequence I used this method in most of my early experiments, before finding the equally good adjustment described in the preceding section.

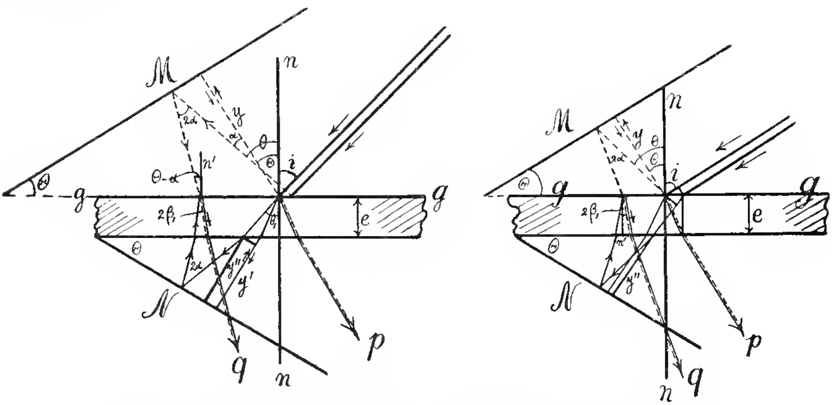


FIG. 24.—Diagrams showing interferences of diffracted rays, case $\Theta$ normal to mirrors $M$ and $N$; case $\theta$ oblique to mirrors. Double incidence.

**39. Elementary theory.**—To find the path differences figs. 24 and 25 may be consulted. In both the grating face is shown at $gg$, the glass plate being $e$ cm. in thickness below it, and $n$ is the normal to the grating. $M$ and $N$ are the two opaque mirrors, each at an angle $\Theta$ to the face of the grating. Light is incident on the right at an angle $i$ nearly 45° In both figures the rays $y_m$ and $y_n$ (air-paths) diffracted at an angle $\Theta$ in air, are reflected normally from the mirrors $M$ and $N$ respectively and issue toward $p$ for interference. The rays $y_n$ (primed in figure) pass through glass. Both figures also contain two component rays diffracted at an angle $\theta$ in air, where $\theta - \Theta = \alpha$, and reflected obliquely at the mirrors $M$ and $N$, thus inclosing an angle $2\alpha$ in air and $2\beta_1$ in glass, and issuing toward $q$. These component rays are drawn in full and dotted, respectively. In fig. 24 there are two incident rays for a single emergent ray, in fig. 25 a single incident ray for two emergent rays interfering in the telescope. The treatment of the two cases is different in detail; but as the results must be the same, they corroborate each other.

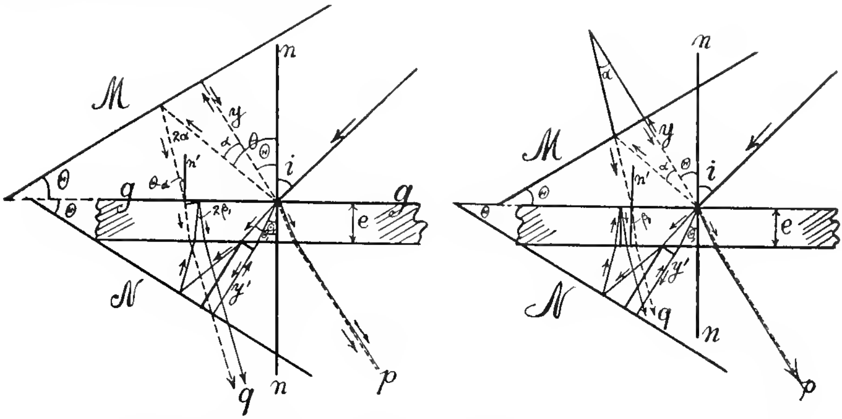


FIG. 25.—Diagrams showing interferences of diffracted rays, case $\Theta$ normal to mirrors $M$ and $N$; case $\theta$ oblique to mirrors. Single incidence.

The notation used is as follows: Let $e$ be the normal thickness of the grating, $e'$ the effective thickness of the compensator when used. Let distance measured normal to the mirror be termed $y$, $y_n$ and $y_m$ being the component air-paths passing on the glass and on the air side of the grating $gg$, so that $y_m > y_n$. Let $y = y_m - y_n$ be the air-path difference. Similarly let distances $z$ be measured normal to the grating, so that $z$ may refer to displacements of the grating.

Let $i$ be the angle of incidence, $r$ the angle of refraction, and $\mu_r$ the index of refraction for the given color, whence $\sin i = \mu_r \sin r$. Similarly if $\Theta$ is the angle of diffraction in air of the $y$ rays and $\Theta_1$ the corresponding angle in glass,

$$\sin \Theta = \mu_\Theta \sin \Theta_1 \tag{1}$$

and if $\theta$ is the angle of diffraction of any oblique ray in air and $\theta_1$ the corresponding angle in glass

$$\sin \theta = \sin (\Theta + \alpha) = \mu_\theta \sin \theta_1 \tag{2}$$

I have here supposed that $\theta > \Theta$, so that $\alpha = \theta - \Theta$ is the deviation of the oblique ray from the normal ray in air. Finally, the second reflection of the oblique ray necessarily introduces the angle of refraction within the glass such that

$$\sin (\Theta - \alpha) = \mu_\theta \sin \beta_1 \tag{3}$$

If $D$ is the grating space we have, moreover,

$$\sin i - \sin \theta = \lambda_\theta / D \quad \text{and} \quad \sin i - \sin \Theta = \lambda_\Theta / D \tag{4}$$

For a displacement, $z$, of the grating, or an equivalent displacement, $y$, of either mirror, the path difference produced in case of the oblique ray will be

$$2y/\cos\alpha = 2z\ (\cos(i-\theta)+\sin(i-\theta))/\cos\alpha\cos i \qquad (5)$$

For normal rays $\cos\alpha = 1$. If as in paragraph 1 the reflection is antecedent

$$i=\theta \qquad\qquad 2y/\cos\alpha = 2z/\cos\alpha\cos i$$

**40. Equations for the present case.**—From a solution of the triangles, preferably in the case for single incidence, as in fig. 25, the air-path of the upper oblique component ray at a deviation $\alpha$ is

$$2y_m\cos\theta/\cos(\theta-\alpha)$$

The air-path of the lower component ray is

$$2\cos\theta\ (y_n - e\sin\theta\ (\tan\theta_1 - \tan\Theta_1))/\cos(\theta-\alpha)$$

The optic path of this (lower) ray in glass as far as the final wave front in glass at $\beta_1$ is

$$\mu_\theta e(1/\cos\theta_1 + 1/\cos\beta_1)$$

The optic path of the upper ray as far as the same wave front in glass is

$$\mu_\theta\sin\beta_1\left\{2\frac{\sin\alpha}{\cos(\theta-\alpha)}(y_m - y_n - e\sin\theta(\tan\theta_1-\tan\Theta_1)) - e(\tan\theta_1-\tan\beta_1)\right\} \qquad (6)$$

Hence the path difference between the lower and the upper ray as far as the final wave front is, on collecting similar terms,

$$2(y_n-y_m)\left(\frac{\cos\theta}{\cos(\theta-\alpha)}+\frac{\sin\alpha\sin(\theta-\alpha)}{\cos(\theta-\alpha)}\right)+\mu_\theta e\left(\frac{1}{\cos\theta_1}+\frac{1}{\cos\beta_1}\right)$$

$$+e\sin(\theta-\alpha)(\tan\theta_1-\tan\beta_1)-\frac{2e}{\cos(\theta-\alpha)}(\tan\theta_1-\tan\Theta_1)$$

$$(\sin\theta\cos\theta+\sin\alpha\sin\theta\sin(\theta-\alpha)) \qquad (7)$$

Before reducing further, one may remark that if incident and emergent rays were coincident, the quantity given under (6) would be zero. Hence if this particular $y_n - y_m = y_1$, it follows that

$$2y_1 = 2e\sin\theta(\tan\theta_1-\tan\Theta_1) - \frac{e\cos(\theta-\alpha)}{\sin\alpha}(\tan\theta_1-\tan\beta_1)$$

Hence the particular path difference for this case would be

$$\mu_\theta e(1/\cos\theta_1 + 1/\cos\beta_1) - e\cos\theta(\tan\theta_1-\tan\beta_1)/\cos\alpha$$

which becomes indeterminate when $\alpha = 0$.

To return to path differences, equation (7), the coefficients of $y_m - y_n = y$ (where $y$ is positive) and of $e$ may now be brought together, as far as possible. If the path difference corresponds to $n$ wave-lengths $\lambda_\theta$ we may write after final reduction

$$n\lambda_\theta = -2y\cos\alpha + 2e\mu_\Theta\cos\alpha(1/\cos\Theta_1 - \cos(\theta_1-\Theta_1)/\cos\theta_1) + e\mu_\theta(1+\cos(\theta_1-\beta_1))/\cos\theta_1 \qquad (8)$$

which is the full equation in question for a dark fringe. It is unfortunately very cumbersome and for this reason fails to answer many questions perspicuously. It will be used below in another form.

The equation refers primarily to the horizontal axes of the ellipses only, as $e$ increases vertically above and below this line. The equation may be abbreviated

$$n\lambda_\theta = -2y\cos\alpha + eZ_\Theta + eZ_\theta$$

where $Z_\Theta$ and $Z_\theta$ are the coefficients of $e$ in the equation. In case of a parallel compensator of thickness $e'$ we may therefore write, $y$ being the path difference in air,

$$n\lambda_\theta = -2y\cos\alpha + (e-e')(Z_\Theta - Z_\theta) \qquad (9)$$

If $e=e'$, *i.e.*, for an infinitely thin plate $e=0$,

$$n\lambda_\theta = 2y\cos\alpha \qquad (10)$$

Again for normal rays $y_m$ and $y_n$, $\alpha=0$ and $\Theta_1=\theta_1=\beta_1$. Hence

$$n\lambda_\Theta = -2y + 2e\mu_\Theta/\cos\Theta_1 \qquad (11)$$

and for a parallel compensator of thickness $e'$

$$n\lambda_\Theta = -2y + 2(e-e')\mu_\Theta/\cos\Theta_1 \qquad (12)$$

If $\mu_\Theta = 1 = \mu_\theta$, equation (8) reduces to

$$n\lambda = 2\cos\alpha(y + e/\cos\theta),$$

clearly identical with the case $e=0$ for a different $y$.

TABLE 11.—Table for path difference, $-2(y_m-y_n)\cos\alpha + eZ_\Theta + eZ_\theta = -2y\cos\alpha + eZ$. Light crown glass. $E$ rays normal to mirrors. Grating space, $D$, = .000 351 2 cm. $I=45°$. $\theta = 33° 51'$

| Spectrum lines = | B | D | E | F | G |
|---|---|---|---|---|---|
| $\lambda\times 10^6$ = | 68.7 | 58.93 | 52.70 | 48.61 | 43.08 cm. |
| $\mu_\theta$ = | 1.5118 | 1.5153 | 1.5186 | 1.5214 | 1.5267 |
| $\theta$ = | 30° 46′ | 32° 38′ | 33° 51′ | 34° 40′ | 35° 46′ |
| $\theta_1$ = | 19° 47′ | 20° 51′ | 21° 31′ | 21° 57′ | 22° 30′ |
| $\alpha$ = | − 3° 5′ | − 1° 13′ | 0° 0′ | 0° 49′ | 1° 55′ |
| $\theta_1-\Theta_1$ = | − 1° 44′ | − 0° 40′ | 0° 0′ | 0° 26′ | 0° 59′ |
| $\beta_1$ = | 23° 25′ | 22° 17′ | 21° 30′ | 21° 13′ | 20° 49′ |
| $\theta_1-\beta_1$ = | − 3° 38′ | − 1° 26′ | 0° 0′ | 0° 44′ | 1° 41′ |
| $2\cos\alpha$ = | 1.9970 | 1.9996 | 2.0000 | 1.9998 | 1.9996 cm. |
| $Z_\Theta$ = | .0383 | .0176 | .0000 | − .0095 | − .0219 cm. |
| $Z_\theta$ = | 3.2100 | 3.2404 | 3.2648 | 3.2805 | 3.3038 cm. |
| Path difference,* $n\lambda$ = | $-1.9970y$ $+3.2483e$ | $-1.9996y$ $+3.2580e$ | $-2.0000y$ $+3.2648e$ | $-1.9998y$ $+3.2710e$ | $-1.9996y$ $+3.2819e$ cm. |
| Path difference $2y=3.2648$ cm. $e=1$ cm. $2\Delta y_0$ = | − .0116 | − .0062 | ± .0000 | + .0059 | + .0177 cm. |
| The same for $e=.68$ cm. $2\Delta y_0$ = | − .0079 | − .0042 | ± .0 | + .0040 | + .0120 cm. |
| $2\Delta N_0$ = | − .0107 | − .0056 | ± .0 | + .0049 | + .0156 cm |

* The purpose of these data is merely to elucidate the equations. $\Delta N$ refers to the displacement of either opaque mirror, $M$ or $N$.

In view of the complicated nature of equation (8), I have computed path differences for a typical case of light crown glass,* as shown in table 11, for the Fraunhofer lines $B$, $D$, $E$, $F$, $G$, supposing the $E$ ray to be normal ($\alpha = 0$). The table is particularly drawn up to indicate the relative value of the functions $Z_{\Theta}$ and $Z_{\theta}$. It will be seen that $Z = Z_{\Theta} + Z_{\theta}$ in terms of $\lambda$, is a curve of regular decrease having no tendency to assume maximum or minimum values within the range of $\lambda$, whereas $y \cos \alpha$ passes through a flat maximum for $\alpha = 0$. This is shown in the curves of fig. 26.

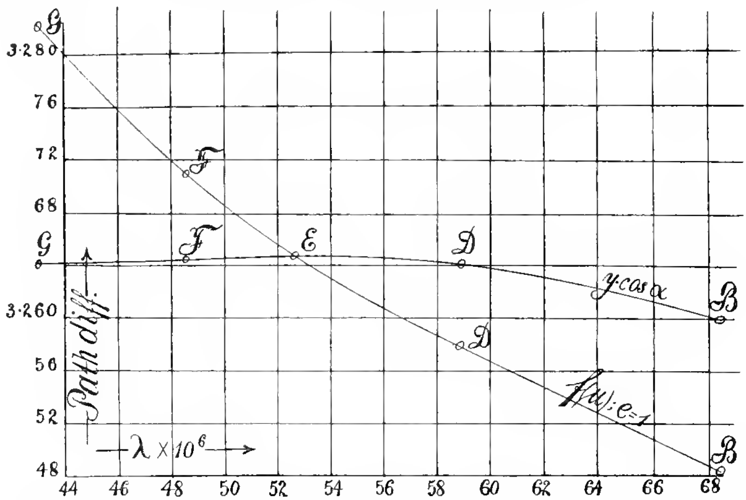


FIG. 26.—Chart showing path difference in centimeters (to be annulled at $E$ line), in terms of wave-length.

The path difference, which is the difference of the ordinates of these curves, thus passes through zero for a definite value of $e$ and $y$, and this would at first sight seem to correspond to the center of ellipses. That it *does not* so correspond will be particularly brought out in the next section, but here this tentative surmise may be temporarily admitted to simplify the descriptions. It is obvious that for a given $e$ the value of $y$ (air-path difference) which makes the total path difference zero, varies with the wave-length, hence on increasing $y$ continuously the ellipses must pass through the spectrum. It is also obvious that, if the grating is reversed, the path difference will change sign, *caet. par.*, and the ellipses will move in a contrary direction, for the same displacements $y$ of the micrometer screw, at the mirror $M$ or $N$, respectively.

If $e = 1$ cm. and $y = 3.2648$ cm., the path difference will be zero for the $E$ ray and (barring further investigation as just stated) one is inclined to place the center of ellipses there. The table shows the residual path differences in the red and blue parts of the spectrum. Fig. 27 has been constructed for

* Taken from Kohlrausch's Practical Physics, 11th edition, 1910, p. 712.

the same condition. It follows, therefore, that in proportion as $e$ is smaller $y$ will be smaller for extinction at the $E$ line. Hence their differences will be smaller and the number of wave-lengths corresponding to the path difference of the Fraunhofer lines will be smaller. In other words, the major axes of the ellipses will be larger. Thus the ellipses will be larger as $e$ is smaller, the limit of enormous ellipses being reached for $e=0$ or $e=e'$ of the compensator.

This result may be obtained to better advantage by reconstructing equation (8), and making the path difference equal to zero for the normal ray. This determines

$$y=e\mu_\Theta/\cos\theta \qquad (13)$$

in terms of $e$, and the path difference now becomes

$$n\lambda_\theta=e\left\{-\mu_\Theta\cos\alpha\cos(\theta_1-\Theta_1)+\mu_\theta(1+\cos(\theta_1-\beta_1))\right\}/\cos\theta_1 \qquad (14)$$

This is zero for $\alpha=0$, $\theta_1=\beta_1=\Theta_1$ at the $E$ line. The other values are given in the table in centimeters and in wave-lengths. Path difference diminishes as $e$; the horizontal axes of the ellipses increase with $e$. If observations are made very near the $E$ line (normal ray) the following approximate form may be used:

$$n\lambda_\theta=(e\mu_\Theta/\cos\theta_1)\left\{2(\mu_\theta/\mu_\Theta-1)+\alpha^2+(\theta_1-\Theta_1)^2-\mu_\theta(\theta_1-\beta_1)^2/2\mu_\Theta\right\} \qquad (15)$$

but this rapidly becomes insufficient unless $\theta_1-\Theta_1$ and $\theta_1-\beta_1$ are very small.

**41. Interferometer.**—If in equation (8), $y$ alone is variable with the order of fringe $n$ while $\alpha$, $\theta$, $\Theta$, $\theta_1$, $\Theta_1$, $\beta_1$, $e$, $\lambda$, $\mu$, are all constant (*i.e.*, if the number of fringes $n$ cross a given fixed spectrum line like the $D$ line, when the mirror is displaced over a distance $y$) it appears that

$$\frac{dy}{dn}=\frac{\lambda_\theta}{2\cos\alpha} \qquad (16)$$

where $\alpha$ refers to the deviation of $\lambda_\theta$ from $\lambda_\Theta$ normal to the mirror. If $\alpha=0$, $dy/dn=0$, the limiting sensitiveness of the apparatus, which appears for the case of normal rays.

If the grating is displaced along $z$

$$\frac{dz}{dn}=\frac{\lambda_\theta}{2\cos\alpha}\,\frac{\cos i}{\cos(i-\Theta)+\sin(i-\Theta)} \qquad (17)$$

where $\cos\alpha=1$ for normal rays. In both cases the displacement per fringe $dy/dn$ and $dz/dn$ vary with the wave-length. Hence if the ellipses are nearly symmetrical on both sides of the center, *i.e.*, if the red and violet sides of the periphery are nearly the same, or the fringes nearly equidistant, the smaller wave-length will move faster than the larger for a given displacement of mirror. In other words, the violet side will pass over a whole fringe before the red and consequently the ellipses, as a whole, must drift in the direction in which violet moves. It is at first quite puzzling to observe the motion of ellipses as a whole in a direction opposed to the motion of the more reddish fringes when these are alone in the field.

**42. Discrepancy of the table.**—The data of table I are computed supposing that the path difference zero corresponds to the center of ellipses. This assumption has been admitted for discussion only and the inferences drawn are qualitatively correct. Quantitatively, however, the displacement of about $\Delta N = .003$ cm. should move the center of ellipses from the *D* to the *E* line of the spectrum, whereas observations show that a displacement of either opaque mirror of about $\Delta N = .01$ cm. is necessary for this purpose; *i.e.*, over three times as much displacement as has been computed. The equation can not be incorrect; hence the assumption that the center of ellipses corresponds to the path difference zero is not vouched for and must be particularly examined. This may be done to greater advantage in connection with the next section, where the conditions are throughout simpler, but the data are of the same order of value.

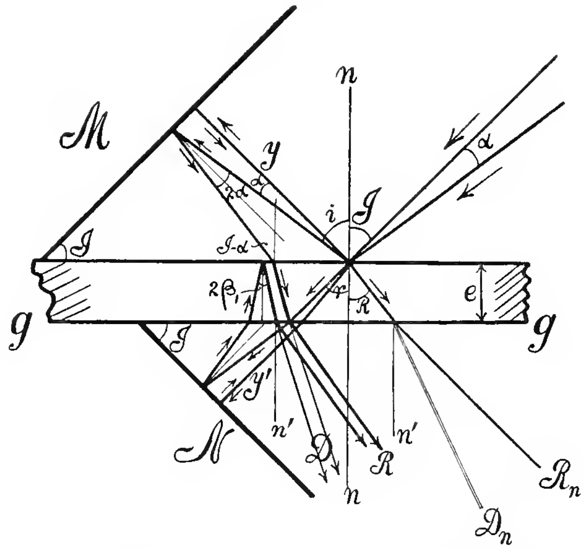


FIG. 27.—Diagram showing interferences of reflected rays, subsequently diffracted. Case *I*, normal to mirrors; case $i = I + \alpha$ oblique to mirrors. Rays *R* refracted, *D* diffracted.

## PART III. DIRECT CASE; REFLECTION ANTECEDENT.

**43. Equations for this case.**—If reflection at the opaque mirrors takes place before diffraction at the grating, the form of the equations and their mode of derivation are similar to the case of paragraph 40, but the variables contained are essentially different. In this case the deviation from the normal ray is due not to diffraction but to the angle of incidence, and the equations are derived for homogeneous light of wave-length $\lambda$ and index of refraction $\mu$.

In fig. 27 let $y_n = y'$ and $y_m = y$ be the air-paths of the component rays, the former first passing through the glass plate of thickness $e$. Let the angle of incidence of the ray be $I$, so that $y_m$ and $y_n$ are returned normally from the mirrors $M$ and $N$, respectively, these being also at an angle $I$ to the plane of the grating. Let $i$ be the angle of incidence of an oblique ray, whose deviation from the normal is $i - I = a$. Let $R$, $r$, and $\beta_1$ be angles of refraction such that

$$\sin i = \sin (I + a) = \mu \sin r \qquad \sin I = \mu \sin R \qquad \sin (I - a) = \mu \sin \beta_1 \quad (18)$$

The face of the grating is here supposed to be away from the incident ray, as shown at $gg$ in the figure.

TABLE 12.—Path difference, $-2(y_m - y_n)\cos a + eZ_1 - eZ_2 + eZ_3$. Light crown glass. $a = 3°$ throughout. Grating space .000351 cm. $I = 45°$. $e = 1$ cm.

| Spectrum lines | B | D | E | F | G |
|---|---|---|---|---|---|
| $\lambda \times 10^6 =$ | 68.7 | 58.93 | 52.70 | 48.61 | 43.08 cm. |
| $\mu =$ | 1.5118 | 1.5153 | 1.5186 | 1.5214 | 1.5267 |
| $R =$ | 27° 53′ | 27° 49′ | 27° 45′ | 27° 42′ | 27° 35′ |
| $r =$ | 29° 26′ | 29° 22′ | 29° 18′ | 29° 14′ | 29° 8′ |
| $\beta_1 =$ | 26° 16′ | 26° 12′ | 26° 8′ | 26° 5′ | 26° 0′ |
| $a =$ | 3° 0′ | 3° 0′ | 3° 0′ | 3° 0′ | 3° 0′ |
| $r - R =$ | 1° 33′ | 1° 33′ | 1° 33′ | 1° 33′ | 1° 33′ |
| $r - \beta_1 =$ | 3° 10′ | 3° 10′ | 3° 10′ | 3° 9′ | 3° 8′ |
| $Z_1 =$ | 3.4160 | 3.4218 | 3.4272 | 3.4318 | 3.4403 cm. |
| $Z_2 =$ | 656 | 714 | 767 | 808 | 896 cm. |
| $Z_2 =$ | 689 | 647 | 799 | 841 | 928 cm. |
| Path difference, $a = 3°$, $e = 1$ cm., $y = 1$ cm. $n\lambda =$ | −1.9992 +3.4193 | −1.9992 +3.4252 | −1.9992 +3.4304 | −1.9992 +3.4352 | −1.9992 +3.4436 |
| If path difference is annulled at $E$ line, $a = 3°$, $e = 1$ cm. $2\Delta y'_0 =$ | − .0111 | − .0052 | ±.0 | + .0048 | + .0132 |
| The same, if $a = 0°$, $e = 1$ cm. $2\Delta y'_0 =$ | − .0111 | − .0052 | ±.0 | + .0048 | + .0132 |

The data are merely intended to elucidate the equations.
The values $Z$ are nearly equal. So also the cases for $a = 3°$ and $a = 0°$.

Fig. 28 has been added to accentuate the symmetrical conditions when a compensator parallel to the grating and of the same thickness is employed.

Then it follows as in paragraph 40, *mutatis mutandis*, that the path difference is (if $y = y_m - y_n$)

$$n\lambda = -2y \cos a + \mu e \left\{ \frac{2 \cos a}{\cos R} - \frac{2 \cos a \cos (r - R)}{\cos r} + \frac{1 + \cos (r - \beta_1)}{\cos r} \right\} \quad (19)$$

$$= -2y \cos a + e(Z_1 - Z_2 + Z_3)$$

where $n$ is the order of interference (whole number). This equation is intrinsically simpler than equation (8) since $\mu_r = \mu_R$, as already stated, and since $\alpha$ is constant for all colors, or all values of $\mu$ and $\lambda$, in question. $R$ and $r$ replace $\Theta_1$ and $\theta_1$.

In most respects the discussion of equation (19) is similar to equation (8) and may be omitted in favor of the special interpretations presently to be given. If $\mu = 1$, equation (19) like equation (8) reduces to the case corresponding to $e = 0$, with a different $y$ normal to the grating.

All the colors are superposed in the direct image of the slit, $R_n$ and $R$ in fig. 27, seen in the telescope, and the slit is therefore white. This shows

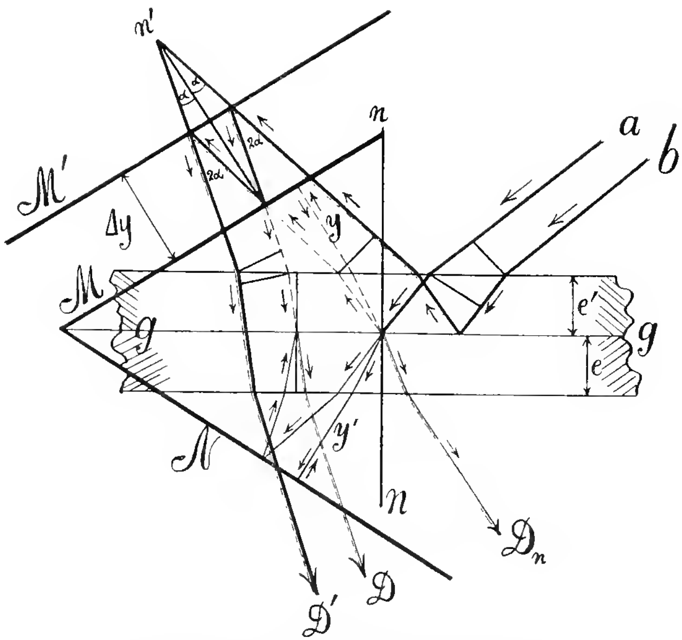


FIG. 28.—Diagram showing symmetrical interference for compensated grating, $gg$. Rays oblique to mirror.

also that prismatic deviation due to the plate of the grating (wedge) is inappreciable. The colors appear, however, when the light of the slit is analyzed by the grating in the successive diffraction spectra, $D_n$ or $D$, respectively. In equation (19) $\mu$ is a function of $\lambda$ and hence of the deviation $\theta$ produced by the grating, since $\sin (I-\alpha) - \sin \theta = \lambda/D$.

The values of equation (19) for successive Fraunhofer lines and for $\alpha = 3°$, have been computed in table 12 for the same glass treated in table 11, the data being similar and in fact of about the same order of value. The feature of this table is the occurrence of nearly constant values $\alpha = i - I$,

$r-R$ and $r-\beta_1$, throughout the visible spectrum. Hence if the following abbreviations be used

$$A=\cos\alpha=.9986 \qquad B=\cos(r-R)=.9996 \qquad C=1+\cos(r-\beta_1)=1.9984$$

$A$, $B$, $C$ are practically functions of $\alpha$ only and do not vary with color or $\lambda$. Furthermore, if the path difference is annulled, at the $E$ line for instance, for the normal ray, since $r=\beta_1=R$, $\alpha=0$, so that $R=R_E$ is the normal angle of refraction,

$$0=-y+2\mu e/\cos R_E$$

and equation (19) reduces to

$$n\lambda=2eA(\mu/\cos R-\mu\cos R_E)+e(C-2AB)\mu/\cos r \tag{20}$$

where $2eA$ and $e(C-2AB)$ are nearly independent of $\lambda$ and the last quantity is relatively small. The two terms of this equation for $e=1$ cm. show about the following variation:

TABLE 13.

| B | D | E | F | G |
|---|---|---|---|---|
| −.0111 | −.0052 | .0 | +.0048 | .0132 |
| −.000009 | −.000004 | .0 | +.000005 | .000013 |

Hence for deviations even larger than $\alpha=3°$, the path difference does not differ practically from the path difference for the normal ray. Thus it follows that the equation

$$n\lambda=-2y+2e\mu/\cos R \tag{21}$$

is a sufficient approximation for such purposes as are here in view.

Finally, for $e=.68$ cm. (the actual thickness of the plate of the grating), $y$ and $N$, the semi-path difference and the displacement of the opaque mirror, will be

TABLE 14.

| | B | D | E | F | G |
|---|---|---|---|---|---|
| $y_0=$ | 1.1630 | 1.1650 | 1.1668 | 1.1686 | 1.1730 |
| $\Delta y_0=$ | − .0038 | − .0018 | .0 | + .0016 | + .0045 |
| $\delta N_0=$ | + .0014 | + .0007 | .0 | − .0005 | − .0018 |
| $\Delta N_0=$ | − .0052 | − .0025 | .0 | + .0021 | + .0063 |

where $\delta N_0$ is the color correction of $\Delta y_0$ and $\Delta N_0=\Delta y_0-\delta N_0$ determines the corresponding displacements of the opaque mirror; or more briefly

$$N_0=y_0-e\mu\tan R\sin R=2e\mu\cos R \tag{22}$$

The data actually found were

| | C | D | E | F |
|---|---|---|---|---|
| $\Delta N_0=$ | −.0148 | −.0093 | .0 | +.0057 |